

Approximate Factor Models for Functional Time Series

Sven Otto*

Institute of Econometrics and Statistics, University of Cologne
and

Nazarii Salish

Department of Economics, Universidad Carlos III de Madrid

February 26, 2025

Abstract

We propose a novel approximate factor model tailored for analyzing time-dependent curve data. Our model decomposes such data into two distinct components: a low-dimensional predictable factor component and an unpredictable error term. These components are identified through the autocovariance structure of the underlying functional time series. The model parameters are consistently estimated using the eigencomponents of a cumulative autocovariance operator and an information criterion is proposed to determine the appropriate number of factors. Applications to mortality and yield curve modeling illustrate key advantages of our approach over the widely used functional principal component analysis, as it offers parsimonious structural representations of the underlying dynamics along with gains in out-of-sample forecast performance.

Keywords: Curve data, functional data analysis, identification, information criterion, forecasting, yield curve modeling

JEL Classification: C32, C38, C55, E43

*Corresponding author: Sven Otto, Institute of Econometrics and Statistics, University of Cologne, Albertus-Magnus-Platz, 50923 Cologne, Germany. Email: sven.otto@uni-koeln.de

1 Introduction

Over the past decades, approximate and dynamic factor models have emerged as powerful tools for analyzing high-dimensional datasets, offering a parsimonious framework that captures the essential underlying structure while filtering out irrelevant parts. These models, first conceptualized by [Chamberlain and Rothschild \(1983\)](#) and expanded upon by [Forni et al. \(2000\)](#), [Stock and Watson \(2002a,b\)](#), and [Bai \(2003\)](#), have become fundamental tools in areas such as economic forecasting, monetary policy analysis, psychology, environmental and social sciences. For comprehensive reviews, see [Bai and Ng \(2008\)](#), [Breitung and Choi \(2013\)](#), and [Stock and Watson \(2016\)](#).

Building on the success of these models in handling high-dimensional data, the generalization of factor modeling techniques to functional or infinite-dimensional data structures has gained significant attention. This transition to functional data analysis (FDA) is a natural extension, as this field focuses on datasets consisting of continuous curves or functions, as discussed extensively in [Ramsay and Silverman \(2005\)](#), [Horváth and Kokoszka \(2012\)](#), [Hsing and Eubank \(2015\)](#), and [Kokoszka and Reimherr \(2017\)](#). FDA is particularly valuable in economic applications, where data often take functional forms, such as term structures of bond yields, credit default swaps, income profiles, and inflation expectations, for which conventional multivariate methods may prove overly restrictive or inadequate. In this paper, we contribute to the literature on factor models for functional data by proposing a novel approximate factor model that explicitly models the dynamics of time-dependent functional data (or functional time series).

The study of factor models in FDA has seen significant progress in recent years. Early contributions focused on generalizing classical factor models to the functional setting. For instance, [Hays et al. \(2012\)](#) and [Liebl \(2013\)](#) introduced functional factor models with a discrete error component, while [Hörmann and Jammoul \(2022, 2023\)](#) and [Ofner and Hörmann \(2024\)](#) demonstrated how discretely observed functional data follow an approximate factor model structure. These works primarily utilized the functional counterpart of principal component analysis (PCA), building on directions of maximal variability for

factor identification. The same PCA-based approach has been extended to functional time series. For example, [Hyndman and Shang \(2009\)](#) and [Aue et al. \(2015\)](#) applied PCA techniques to model and forecast functional time series, while further extensions have addressed challenges related to nonstationarity and long-range dependence (see, e.g., [Chang et al. 2016](#), [Li et al. 2020](#), and [Salish and Gleim 2019](#)). More recent contributions, such as [Hallin et al. \(2023\)](#) and [Tavakoli et al. \(2023\)](#), have refined these methods, identifying factors asymptotically through panel structures of large functional time series datasets. In addition, Bayesian methods have also offered a rich set of tools for modeling factors in functional datasets both cross-sectional and time series (e.g., [Montagna et al. 2012](#), [Kowal et al. 2017](#), and [Kowal and Canale 2023](#)).

The identification and estimation of factors in functional data analysis typically relies on selecting directions of highest variability, typically obtained through the functional adaptation of PCA. While this approach effectively reduces dimensionality, the resulting factors do not necessarily capture all temporal dependencies or reflect predictability, both of which are integral to functional time series analysis. As argued by [Forni et al. \(2000\)](#), [Panaretos and Tavakoli \(2013\)](#) and [Hörmann et al. \(2015\)](#), focusing solely on variability can lead to an incomplete representation of the data’s dynamic structure, potentially overlooking important serial dependencies. Our paper addresses this limitation by complementing and extending existing methodologies to develop a factor model tailored specifically for functional time series. In this framework, factors are identified based on their contribution to the dynamic and predictive structure of the data, rather than directions of maximal variability.

Similar to existing factor models, our approach decomposes a functional time series into two distinct components: (i) a low-dimensional *factor component* and (ii) a remainder term, referred to as an *error component*. The key distinction lies in how the factor component is derived in our framework. Rather than relying on directions of maximal variability identified through PCA, our method extracts the factor component from the autocovariance structure of the functional time series to reflect serial dependencies and

predictability. This departure from conventional factor analysis enables a better characterization of the temporal dynamics inherent in functional time series. Our methodology is related to those proposed by [Pena and Box \(1987\)](#), [Bathia et al. \(2010\)](#), [Lam and Yao \(2012\)](#), and [Diks and Wouters \(2023\)](#). Consequently, the factors and error components in our model can also be interpreted as *predictable* and *unpredictable*, respectively, reflecting their roles in characterizing the process dynamics. The term “approximate” in the model’s name stems from the allowance for correlations between values at different domain points of the error term, consistent with the terminology introduced by [Chamberlain and Rothschild \(1983\)](#).

Our construction also changes the role and structure of the error component. The primary requirement to the error component is to not carry any relevant information about dynamics of the original functional time series. This, in turn, allows us to relax the typical restrictions imposed in conventional factor models on the error term, allowing for more flexibility. First, the eigenvalues of both the factor and error components can be of comparable magnitude. Second, as an approximate factor model, it permits non-negligible correlations across different domain points of the error function, even asymptotically. This stands in contrast to conventional models, which assume lower magnitude errors and only weak correlations, crucial for separating the factor component from the error one. Finally, in our framework, the factor and error components may exhibit weak cross-correlations, accommodating various forms of nonstationarity and heteroskedasticity.

Following the development of this new factor modeling framework for functional time series, the second main contribution of this paper is to ensure both theoretical rigor and practical applicability. We develop a consistent estimation procedure for the model’s primitives, such as the autocovariance structure, and address the challenge of estimating the factor component’s dimension, which is typically unknown and must be inferred from the data. To tackle this challenge, we propose an information criterion, drawing from traditional solution in factor modeling literature (e.g., [Bai and Ng 2002](#); [Hallin and Liška 2007](#)). Our criterion is based on the prediction error curve and assumes that the factor

component follows a vector autoregressive (VAR) process with an unknown number of lags. We incorporate a carefully designed penalty term in the criterion to mitigate over-selection, ensuring consistent estimates for both the number of factors and the lag order under mild theoretical assumptions. All proposed estimation procedures are available in our R-package¹.

Finally, to illustrate the practical utility of our model, we apply it to mortality and yield curve modeling and forecasting. In both applications, we compare our approach with functional PCA, which has arguably become the main applied workhorse model in functional time series analysis since the seminal work of [Aue et al. \(2015\)](#). Additionally, for yield curves, we benchmark our model against the widely used dynamic Nelson-Siegel model, as reviewed in [Diebold and Rudebusch \(2013\)](#). Our main findings highlight the importance of a careful structural representation of process dynamics – that is, reducing the dimensionality of the original process in a meaningful way by extracting factors that drive the dynamics rather than merely capturing variability. For instance, in the case of mortality rates, while the first three factors in our framework closely resemble those identified by PCA, the remaining factors differ. This distinction proves important, as selecting factors based on their role in driving dynamics rather than explaining variability leads to improved forecasting performance. In the case of yield-curve modeling, our results indicate that the number of factors required to capture yield curve dynamics varies over time, with more factors needed during periods of economic uncertainty than in stable periods. These findings suggest that yield curves have a richer and more adaptive dynamic structure than typically considered in the literature.

The paper is structured as follows: Section 2 develops the approximate functional factor model, providing detailed discussions on all necessary assumptions and the identification of its components. In Section 3, we introduce the estimator for the functional component, discuss the information criterion for jointly estimating the number of factors and their dynamics, and show their consistency. We also provide guidance on practical implementation. Section 4 presents a Monte Carlo simulation to assess the model’s per-

¹<https://github.com/ottosven/dffm>

formance and the proposed estimation methods in finite samples. In Section 5, we apply the method to mortality rate and yield curves. Finally, Section 6 concludes the paper.

To ease the readability of the paper, we collect the key notations below. Consider $H = L^2([a, b])$, the space of square-integrable functions $f : [a, b] \rightarrow \mathbb{R}$ satisfying $\int_a^b f(r)^2 dr < \infty$ for $a < b$. H forms a Hilbert space equipped with the inner product $\langle f, g \rangle = \int_a^b f(r)g(r)dr$ and the norm $\|f\| = \sqrt{\langle f, f \rangle}$, for $f, g \in H$. Any square-integrable kernel function $\rho : [a, b] \times [a, b] \rightarrow \mathbb{R}$ defines an integral operator $\mathcal{R} : H \rightarrow H$, $f(\cdot) \mapsto \int_a^b \rho(\cdot, s)f(s)ds$ with squared Hilbert-Schmidt norm $\|\mathcal{R}\|_{\mathcal{S}}^2 = \int_a^b \int_a^b \rho(r, s)^2 ds dr < \infty$. The image space of \mathcal{R} is $Im(\mathcal{R}) = \{g \in H : g(r) = \int_a^b \rho(r, s)f(s)ds \text{ for some } f \in H\}$, and the rank of \mathcal{R} is the dimension of its image space. An eigenvalue-eigenfunction pair (ξ, v) of \mathcal{R} satisfies $\int_a^b \rho(r, s)v(s)ds = \xi v(r)$, for all $r \in [a, b]$. If $\rho(r, s)$ is symmetric and positive semi-definite, all eigenvalues are real, and eigenfunctions associated with distinct eigenvalues are orthogonal. The adjoint operator \mathcal{R}^* of \mathcal{R} is the integral operator with kernel function $\rho^*(r, s) = \rho(s, r)$. See [Hsing and Eubank \(2015\)](#), Sections 3 and 4, for a detailed exposition of the relevant operator theory. To clarify vector and matrix norms, we use $\|\cdot\|_2$ for the Euclidean vector norm and $\|\cdot\|_M$ for the compatible Frobenius matrix norm.

2 The Approximate Functional Factor Model

We consider a time series of curves $Y_1(r), \dots, Y_T(r)$ defined on the domain $r \in [a, b]$. Our main goal is to develop a framework that is capable of capturing the low-dimensional dynamic behavior of the given functional time series. To achieve this, we employ a general factor model framework:

$$\begin{aligned} Y_t(r) &= \mu(r) + \sum_{l=1}^K F_{l,t} \psi_l(r) + \epsilon_t(r), \\ &= \mu(r) + (\Psi(r))' F_t + \epsilon_t(r), \quad t = 1, \dots, T, \quad r \in [a, b]. \end{aligned} \quad (1)$$

Here, $F_t = (F_{1,t}, \dots, F_{K,t})'$ represents the $K \times 1$ vector of factors driving the dynamic part of $Y_t(r)$, while the error term $\epsilon_t(r)$ carries no relevant serial dependence signal, and $\mu(r)$ is

the standard intercept function. The vector $\Psi(r) = (\psi_1(r), \dots, \psi_K(r))'$ collects K loading functions determining how each factor contributes to the curve series. All components of this model, including the number of factors, K , the vector of loading functions, $\Psi(r)$, and the factors, F_t , are unobserved. To properly identify their role and estimate them, an additional set of conditions is necessary, which we discuss in detail below.

We begin by separating the factor component from the error term, which is a fundamental step in our modeling approach. Central to this step is the concept of serial dependence, which allows us to isolate the low-dimensional dynamic factor component from the noise. This concept is formalized through a set of restrictions outlined in the following assumption:

Assumption 1. *Model (1) holds true with*

(a) $E[\epsilon_t(r) \mid Y_{t-1}, Y_{t-2}, \dots] = 0$ for all t and $r \in [a, b]$;

(b) $E[F_t] = 0$ for all t , and for some integer $q_0 \geq 1$, the $K \times K$ matrix

$$M := \sum_{\tau=1}^{q_0} \int_a^b (M_\tau(s))(M_\tau(s))' ds$$

is positive definite, where $M_\tau(s) := \lim_{T \rightarrow \infty} T^{-1} \sum_{t=\tau+1}^T E[F_t Y_{t-\tau}(s)]$;

(c) ψ_1, \dots, ψ_K are linearly independent and continuous functions.

By Assumption 1(a), the error term ϵ_t has no correlation with lagged Y_t , implying that it cannot be predicted from the past observations of Y_t . In contrast, the factors globally correlate with at least one lag of the original process, Y_t , as specified in Assumption 1(b). To be more specific, the positive definiteness of the matrix M , implies that

$$\lim_{T \rightarrow \infty} \sum_{\tau=1}^{q_0} \int_a^b \left(\frac{1}{T} \sum_{t=1}^T E[F_{l,t} Y_{t-\tau}(r)] \right)^2 dr > 0,$$

ensuring that the global covariance between $F_{l,t}$ and $Y_{t-\tau}$ is non-zero for any $l = 1, \dots, K$ for at least one lag $\tau = 1, \dots, q_0$, and there is no cancellation of this covariance by the

integration. To ensure broad applicability of our framework, we adopt the concept of global covariance, as defined by [White \(2001\)](#), (i.e., $\lim_{T \rightarrow \infty} T^{-1} \sum_{t=\tau+1}^T E[F_t Y_{t-\tau}(r)]$ is used instead of $E[F_t Y_{t-\tau}(r)]$). This concept accommodates potential heteroskedasticity and local nonstationarities within the original process Y_t , which are common in economic applications. The role of q_0 is similar to that of portmanteau tests for autocorrelation, ensuring each factor correlates with at least one of the first q_0 lags of Y_t . [Lam and Yao \(2012\)](#) and [Zhang et al. \(2019\)](#) argue that a small q_0 is sufficient in practice, and in non-seasonal setups, $q_0 = 1$ can be chosen. It is important to note that q_0 serves only to identify the factor model parameters and does not specify the type or features of temporal dependencies imposed on the process Y_t . Finally, from Assumption [1\(a\)](#) and [\(b\)](#), the intercept $\mu(r)$ is identified as the mean function $E[Y_t(r)]$. This renders the first two terms in [\(1\)](#), expressed as

$$\chi_t(r) := \mu(r) + (\Psi(r))' F_t, \quad (2)$$

predictable from the original process $Y_t(r)$, justifying the terminology introduced in the introduction section for the corresponding parts as *predictable* and *unpredictable*.

The set of loading functions forms a basis for the factor space $H_F := \text{span}(\psi_1, \dots, \psi_K)$, where Y_t exhibits autocovariances. The linear independence of the loading functions, as dictated by Assumption [1\(c\)](#), implies that H_F is K -dimensional. Essentially, this indicates the presence of K distinct directions along which Y_t displays temporal dependence. Consequently, identifying H_F plays a pivotal role in understanding the autocovariance structure of Y_t , leading to the subsequent step in our model: identifying the loading functions and determining their number.

The structure of the global autocovariance of Y_t depends solely on the structure of the autocovariance of the factors and the directions represented by the loadings. According

to our model (1), the global τ -th order autocovariance function is expressed as:

$$c_\tau(r, s) := \lim_{T \rightarrow \infty} \frac{1}{T} \sum_{t=\tau+1}^T \text{Cov}[Y_t(r), Y_{t-\tau}(s)] = (\Psi(r))'(M_\tau(s)). \quad (3)$$

Here, $c_\tau(r, s)$ is the kernel function of the global integral autocovariance operator C_τ . Heuristically, each autocovariance C_τ for $\tau = 1, \dots, q_0$ captures some, but not necessarily all, of the directions of interest across which the original series exhibits serial dependence. This fact follows from (3), as these directions are linear combinations of ψ_1, \dots, ψ_K . Specifically, the directions captured by C_τ are represented by its image, $\text{Im}(C_\tau)$, the space spanned by the right-singular functions of C_τ . Following standard results on singular value decomposition, these functions are the orthonormal eigenfunctions of the positive semi-definite operator $C_\tau C_\tau^*$, where C_τ^* denotes the adjoint operator of C_τ . Since $\text{Im}(C_\tau)$ may only capture a subset of the relevant directions (i.e., $\text{Im}(C_\tau) \subset H_F$), a combined analysis of such operators for $\tau = 1, \dots, q_0$ becomes necessary.

We adopt the approach used in Bathia et al. (2010), introducing a cumulative operator $D = \sum_{\tau=1}^{q_0} C_\tau C_\tau^*$, with its kernel function given by:

$$d(r, s) := \sum_{\tau=1}^{q_0} \int_a^b c_\tau(r, q) c_\tau(s, q) dq = (\Psi(r))' M(\Psi(s)).$$

The cumulative autocovariance operator D is symmetric with $\text{Im}(D) = \text{Im}(D^*) = H_F$ and $\text{rank}(D) = K$, as implied by Assumption 1(b) and (c). By construction, its collection of ordered orthogonal eigenfunctions, denoted here as d_1, \dots, d_K , span the entire space H_F , thereby capturing all directions in which Y_t exhibits serial dependence. However, the loading functions ψ_1, \dots, ψ_K also span H_F , indicating that they are linear combinations of d_1, \dots, d_K . Hence, while H_F can be properly identified through d_1, \dots, d_K , the loadings are identified up to some rotation of these eigenfunctions.

To achieve the exact identification, we resort here to the solution routinely used in conventional factor analysis, where loadings are assumed to be orthonormal and factors have a diagonal covariance matrix (see, e.g., Stock and Watson 2002a, and Bai and Ng

2013). Unlike classical factor analysis, we impose a diagonal structure on the positive definite matrix M , as our model aims to identify factors based on the cumulative autocovariance rather than the highest variability. This leads us to the next set of restrictions outlined in the following assumption:

Assumption 2.

(a) The loading functions ψ_1, \dots, ψ_K satisfy $\|\psi_l\| = 1$ and $\langle \psi_l, \psi_m \rangle = 0$ for $l \neq m$.

(b) The matrix M is diagonal with $M = \text{diag}(\lambda_1, \dots, \lambda_K)$ and $\lambda_1 > \dots > \lambda_K > 0$.

These conditions fix the rotation of the loading functions in the factor space H_F , ensuring their exact identification. To see this, by Assumption 2(b), the kernel function of the operator D satisfies

$$d(r, s) = (\Psi(r))' M (\Psi(s)) = \sum_{l=1}^K \lambda_l \psi_l(r) \psi_l(s),$$

implying that $\lambda_1, \dots, \lambda_K$ are the descendingly ordered nonzero eigenvalues of D . Then the loadings ψ_1, \dots, ψ_K are identified as the eigenfunctions d_1, \dots, d_K of operator D up to a sign change and their number as the rank of this operator. It's noteworthy that ψ_1, \dots, ψ_K as eigenfunctions satisfy certain optimality properties given in the proposition below:

Proposition 1. Under Assumptions 1–2, for any $l = 1, \dots, K$,

$$\psi_l = \underset{\substack{f \in \text{span}(\psi_1, \dots, \psi_{l-1})^\perp \\ \|f\|=1}}{\text{argmax}} \lim_{T \rightarrow \infty} \sum_{\tau=1}^{q_0} \int_a^b \left(\frac{1}{T} \sum_{t=\tau+1}^T E[\langle Y_t - \mu, f \rangle Y_{t-\tau}(r)] \right)^2 dr,$$

and,

$$\lim_{T \rightarrow \infty} \sum_{\tau=1}^{q_0} \int_a^b \left(\frac{1}{T} \sum_{t=\tau+1}^T E[\langle Y_t - \mu, g \rangle Y_{t-\tau}(r)] \right)^2 dr = 0, \quad \text{for all } g \in H_F^\perp.$$

According to Proposition 1, the projection of $Y_t - \mu$ onto H_F , as defined by

$$Y_t^*(r) := \mu(r) + \sum_{l=1}^K \langle Y_t - \mu, \psi_l \rangle \psi_l(r), \tag{4}$$

captures all components of the functional time series that correlate with its past q_0 lags. The projection coefficient $\langle Y_t - \mu, \psi_1 \rangle$ is optimal in the sense that there are no other projection coefficients that have a higher dependency with these lags. The second projection coefficient $\langle Y_t - \mu, \psi_2 \rangle$ is optimal among all projections orthogonal to ψ_1 , and this pattern continues with subsequent coefficients.

As the loadings ψ_1, \dots, ψ_K are deterministic, the dynamic nature of Y_t can be equivalently represented by the $K \times 1$ vector $F_t^* := (F_{1,t}^*, \dots, F_{K,t}^*)'$, where $F_{l,t}^* := \langle Y_t - \mu, \psi_l \rangle$ are the scores of projection (4) for $l = 1, \dots, K$. Further from model (1), we deduce:

$$F_{l,t}^* = \langle Y_t - \mu, \psi_l \rangle = F_{l,t} + \langle \epsilon_t, \psi_l \rangle. \quad (5)$$

This implies that the factors $F_{l,t}$ are partially identified as $F_{l,t}^*$, up to an unpredictable noise error term $\langle \epsilon_t, \psi_l \rangle$. In other words, under Assumptions 1 and 2, the factor model (1) cannot be distinguished from its orthogonalized form:

$$Y_t(r) = \mu(r) + (\Psi(r))' F_t^* + \epsilon_t^*(r),$$

where $\epsilon_t^*(r) := \epsilon_t(r) - \sum_{l=1}^K \langle \epsilon_t, \psi_l \rangle \psi_l(r)$.

Achieving complete factor identification may require imposing further restrictions on the model. For example, one could assume that ϵ_t solely takes values in H_F^\perp (the orthogonal complement of H_F), implying $F_t^* = F_t$ for all t . Alternatively, a weaker version of this restriction, where the variance of ϵ_t in H_F is asymptotically negligible, could be considered, as often done in conventional factor literature. Additionally, adopting smoothness versus roughness type of restrictions could help to separate factors from the part of the error term in H_F , as proposed in Descary and Panaretos (2019). We refrain from imposing additional restrictions in this study to maintain the generality of our framework and proceed with partially identified factors $F_{l,t}^*$ in the subsequent analysis. Furthermore, all results presented in the subsequent sections regarding the estimation of the model's primitives, the subspace H_F and the suggested information criterion for the number of

factors, K , do not require complete factor identification.

While Assumptions 1 and 2 establish the necessary restrictions to identify the role of each unobserved component in our model, additional constraints are required to specify time dependencies allowed for the process Y_t as well as factors. These restrictions are required to establish the asymptotic properties of the estimators proposed in the subsequent sections.

Assumption 3.

(a) *The modified factors F_t^* follow a K -variate $VAR(p)$ model, described by $A(L)F_t^* = \eta_t$, where $A(L) = I_K - \sum_{i=1}^p A_i L^i$ is the lag polynomial with L as the backshift operator. It is assumed that $\det(A(z))$ has all roots outside the unit circle and $A_p \neq 0$. The innovations vector η_t forms a martingale difference sequence with zero conditional mean and a positive definite global conditional covariance matrix Σ_η , i.e., $E[\eta_t \mid \eta_{t-1}, \eta_{t-2}, \dots] = 0$ and $\lim_{T \rightarrow \infty} T^{-1} \sum_{t=1}^T E[\eta_t \eta_t' \mid \eta_{t-1}, \eta_{t-2}, \dots] = \Sigma_\eta$. Moreover, $\sup_{t \in \mathbb{Z}} E[\eta_{l,t}^4] < \infty$ for any $l = 1, \dots, K$, and*

$$\lim_{T \rightarrow \infty} \sup_{i_1, i_2, i_3, i_4 \in \mathbb{N}} \frac{1}{T} \left| \sum_{t,s=1}^T \text{Cov}[\eta_{l_1, t-i_1} \eta_{l_2, t-i_2}, \eta_{l_3, s-i_3} \eta_{l_4, s-i_4}] \right| < \infty$$

for all $l_1, l_2, l_3, l_4 \in \{1, \dots, K\}$, where $\eta_{l,t}$ denotes the l -th element of η_t .

(b) *The error term satisfies $\sup_{r \in [a,b]} \sup_{t \in \mathbb{Z}} E[(\epsilon_t^*(r))^4] < \infty$ and*

$$\lim_{T \rightarrow \infty} \sup_{\substack{s \in [a,b] \\ h \geq 0}} E \left[\left\| \frac{1}{\sqrt{T}} \sum_{t=h+1}^T F_t^* \epsilon_{t-h}^*(s) \right\|_2 \right] < \infty.$$

Vector autoregressions, as described in Assumption 3(a), offer a general and convenient framework to model the time-dependencies of factors and allows us to estimate the loadings and the number of factors with parametric rates. Under Assumption 3, the functional time series Y_t is not required to be strictly or covariance stationary. However, in combination with Assumption 1(a), Y_t is globally covariance stationary. Alternative weak dependence assumptions may be based on strong mixing conditions or L^4 - m -approximability

(see [Hörmann and Kokoszka 2010](#)). Weak dependencies between factors and lagged errors, similar to those in [Bai \(2003\)](#), are allowed by Assumption 3(b) as long as they become sufficiently small in the limit.

Remark 1. Throughout this paper, we assume that the curves Y_1, \dots, Y_T are already given as fully observed elements of H . In practice, however, the data is typically only available in the form of high-dimensional vectors, and additional preprocessing steps are needed to transform the discrete observations into functions. This problem has been extensively studied in the literature on functional data analysis and is well understood. The most commonly applied techniques are based on basis expansions (see [Ramsay and Silverman 2005](#)) or a conditional expectation approach (see [Yao et al. 2005](#)). In the empirical part of our paper, we consider curve data that is equidistantly observed with more than $N = 100$ observations per curve, where integrals are approximated by numerical integration. [Hall et al. \(2006\)](#), [Li and Hsing \(2010\)](#), [Zhang and Wang \(2016\)](#), and [Kneip and Liebl \(2020\)](#) showed that mean functions, eigenvalues, and eigenfunctions can be estimated at the same parametric convergence rate as if the curves were fully observed if the discrete data is observed densely enough with $N/T^{1/4} \rightarrow \infty$ and if the second derivatives of the curves are continuous.

3 Estimation

The previous section’s identification results demonstrate that all unobserved components in the model can be expressed using the global autocovariances of the functional time series Y_t . Most of these components can be estimated using method of moments estimators by substituting population moments with sample equivalents. Section 3.1 elaborates on the consistency of these estimators. However, estimating the number of factors presents a more challenging task, which is addressed in Section 3.2, where we introduce an information criterion for consistently determining the number of factors. Finally, Section 3.3 provides practical implementation guidelines, including an estimation and prediction algorithm.

3.1 Estimation of parameter functions

Consider the sample mean function

$$\hat{\mu}(r) = \frac{1}{T} \sum_{t=1}^T Y_t(r),$$

the τ -th order sample autocovariance function

$$\hat{c}_\tau(r, s) := \frac{1}{T} \sum_{t=\tau+1}^T (Y_t(r) - \hat{\mu}(r))(Y_{t-\tau}(s) - \hat{\mu}(s)),$$

and the sample counterpart of the cumulative autocovariance function $d(r, s)$ given as

$$\hat{d}(r, s) = \sum_{\tau=1}^{q_0} \int_a^b \hat{c}_\tau(r, q) \hat{c}_\tau(s, q) dq. \quad (6)$$

The integral operators with kernel functions $\hat{c}_\tau(r, s)$ and $\hat{d}(r, s)$ are denoted as \hat{C}_τ and \hat{D} , respectively. Let $\hat{\lambda}_1 \geq \dots \geq \hat{\lambda}_T \geq 0$ be the eigenvalues of \hat{D} , and let $\hat{\psi}_1, \dots, \hat{\psi}_T$ be corresponding orthonormal eigenfunctions. In practice, the eigenequation and the integral in (6) are computed by numerical integration. A ready-to-use implementation is provided in our accompanying R package.

Theorem 1. *Under Assumptions 1–3,*

- (a) $\|\hat{\mu} - \mu\| = O_P(T^{-1/2})$
- (b) $\|\hat{C}_\tau - C_\tau\|_{\mathcal{S}} = O_P(T^{-1/2})$ for all $\tau = 1, \dots, q_0$
- (c) $\|\hat{D} - D\|_{\mathcal{S}} = O_P(T^{-1/2})$
- (d) $|\hat{\lambda}_l - \lambda_l| = O_P(T^{-1/2})$ for all $l = 1, \dots, K$ and $\hat{\lambda}_l = O_P(T^{-1/2})$ for $l > K$.
- (e) $\|\hat{\psi}_l - s_l \psi_l\| = O_P(T^{-1/2})$ for all $l = 1, \dots, K$, where $s_l = \text{sign}(\langle \hat{\psi}_l, \psi_l \rangle)$

Theorem 1 implies that the parameter functions in model (1) are consistently estimated with parametric rates of convergence. To estimate the factors themselves, given the

estimated intercept and loading functions, we use the sample equivalents of the factors in (5), defined as

$$\widehat{F}_{l,t} := \langle Y_t - \widehat{\mu}, \widehat{\psi}_l \rangle, \quad l = 1, \dots, K, \quad t = 1, \dots, T.$$

Using this projection coefficient as our factor estimator is further justified by the least squares principle, as it optimizes the model fit by minimizing

$$\left\| Y_t - \widehat{\mu} - \sum_{k=1}^K f_{k,t} \widehat{\psi}_k \right\|^2 = \sum_{k=1}^K (f_{k,t}^2 - 2f_{k,t} \langle Y_t - \widehat{\mu}, \widehat{\psi}_k \rangle) + \|Y_t - \widehat{\mu}\|^2,$$

where the minimum is attained when $f_{l,t} = \widehat{F}_{l,t}$.

Theorem 1(e) highlights the relevance of the sign $s_l = \text{sign}(\langle \widehat{\psi}_l, \psi_l \rangle)$ for our theoretical analysis, since the signs of the eigenfunctions are unidentified. Conditional on the chosen signs for the eigenfunctions of \widehat{D} , the sign-adjusted quantities $s_l \psi_l$ and $s_l F_{l,t}^* = \langle Y_t - \mu, s_l \psi_l \rangle$ serve as the population equivalents of $\widehat{\psi}_l$ and $\widehat{F}_{l,t}$. However, flipping the signs of the loadings also flips the signs of the factors, so the products $\widehat{F}_{l,t} \widehat{\psi}_l$ and $F_{l,t}^* \psi_l$ remain invariant to sign changes. Together with Theorem 1, a direct consequence is that

$$\frac{1}{T} \sum_{t=1}^T \left\| \sum_{l=1}^K \widehat{F}_{l,t} \widehat{\psi}_l - F_{l,t}^* \psi_l \right\| = O_P(T^{-1/2}),$$

since, for any given $t = 1, \dots, T$, the estimation error $|\widehat{F}_{l,t} - s_l F_{l,t}^*|$ is bounded from above by $\|\mu - \widehat{\mu}\| + \|Y_t - \mu\| \|\widehat{\psi}_l - s_l \psi_l\|$.

3.2 Estimation of the number of factors

To determine the number of factors K , we exploit their dynamic VAR structure, defined in Assumption 3, and construct an information criterion for its selection. The advantage of this approach is that it not only aids in the estimation of K but also provides the opportunity to estimate the number of lags of the VAR structure, which is an essential step for empirical applications.

The temporal dynamics of the curve process Y_t and its latent factors are characterized

by the $K \times pK$ matrix of autoregressive coefficients denoted by $\mathbf{A} = [A_1, \dots, A_p]$, as defined in Assumption 3(a). We employ the standard conditional least squares (LS) estimator to estimate \mathbf{A} . For a selected number of factors J and lags m , the unknown $K \times 1$ vectors F_t^* are replaced with the $J \times 1$ vectors of sample scores $\hat{F}_t^{(J)} = (\hat{F}_{1,t}, \dots, \hat{F}_{J,t})'$. The LS estimator is given by

$$\hat{\mathbf{A}}_{(J,m)} = \hat{\Gamma}_{(J,m)} \hat{\Sigma}_{(J,m)}^{-1} \quad (7)$$

with $\hat{\Gamma}_{(J,m)} = T^{-1} \sum_{t=m+1}^T \hat{F}_t^{(J)} (\hat{\mathbf{x}}_{t-1}^{(J,m)})'$ and $\hat{\Sigma}_{(J,m)} = T^{-1} \sum_{t=m+1}^T \hat{\mathbf{x}}_{t-1}^{(J,m)} (\hat{\mathbf{x}}_{t-1}^{(J,m)})'$, where the stacked vector of lagged sample scores is $\hat{\mathbf{x}}_{t-1}^{(J,m)} = ((\hat{F}_{t-1}^{(J)})', \dots, (\hat{F}_{t-m}^{(J)})')'$. Conditional on the selected number of factors and lags, the one-step ahead curve predictor is expressed as

$$\hat{Y}_{t|t-1}^{(J,m)}(r) = \hat{\mu}(r) + (\hat{\Psi}^{(J)}(r))' \hat{\mathbf{A}}_{(J,m)} \hat{\mathbf{x}}_{t-1}^{(J,m)}, \quad \hat{\Psi}^{(J)}(r) = (\hat{\psi}_1(r), \dots, \hat{\psi}_J(r)),$$

and the corresponding mean squared error (MSE) is given by

$$MSE_T(J, m) = \frac{1}{T-m} \sum_{t=m+1}^T \|Y_t - \hat{Y}_{t|t-1}^{(J,m)}\|^2. \quad (8)$$

Given that $MSE_T(J, m)$ depends on both the number of selected factors and the number of lags, it can be used to construct a consistent information criterion. To achieve this, we first must examine how MSE_T behaves with respect to J and m , considering two sources of uncertainty: one from estimating the model parameter functions and the other from estimating the vector autoregression itself. The model parameter functions that enter MSE_T (i.e., μ and ψ_l) are invariant with respect to J and m and, according to Theorem 1, are estimated with parametric rates of convergence. Hence, it remains crucial to understand how the asymptotic properties of the conditional LS estimator and therefore MSE_T are impacted by a misspecified number of factors and lags.

The population coefficient matrix, \mathbf{A} , and the conditional LS estimator matrix, $\hat{\mathbf{A}}_{(J,m)}$, are of different dimensions. To align the $K \times Kp$ matrix \mathbf{A} with the $J \times Jm$ matrix $\hat{\mathbf{A}}_{(J,m)} = [\hat{A}_1^{(J)}, \dots, \hat{A}_m^{(J)}]$, we transform them into matrices of order $J^* \times J^*m^*$ with $J^* =$

$\max\{J, K\}$ and $m^* = \max\{m, p\}$ by inserting zeros where their dimensions do not match.

Using the completion matrix

$$\mathbf{R}_{J,K} = \begin{cases} [\mathbf{I}_J, \mathbf{0}_{J,K-J}], & \text{if } J < K, \\ \mathbf{I}_J, & \text{if } J \geq K, \end{cases}$$

where $\mathbf{0}_{J,K}$ is the $J \times K$ matrix of zeros and \mathbf{I}_J is the identity matrix, we define the aligned LS estimator

$$\hat{\mathbf{A}}^* = \begin{cases} [\mathbf{R}'_{J,K} \hat{\mathbf{A}}_1^{(J)} \mathbf{R}_{J,K}, \dots, \mathbf{R}'_{J,K} \hat{\mathbf{A}}_m^{(J)} \mathbf{R}_{J,K}, \mathbf{0}_{J^*,(p-m)J^*}], & \text{if } m < p, \\ [\mathbf{R}'_{J,K} \hat{\mathbf{A}}_1^{(J)} \mathbf{R}_{J,K}, \dots, \mathbf{R}'_{J,K} \hat{\mathbf{A}}_m^{(J)} \mathbf{R}_{J,K}], & \text{if } m \geq p. \end{cases}$$

Given that the loadings are only identified and correctly estimated up to a sign change, we condition our notation on the selected signs and consider the sign-adjusted matrices $\tilde{\mathbf{A}}_i = \mathbf{S} \mathbf{A}_i \mathbf{S}$ for $i = 1, \dots, K$, with the sign transformation matrix $\mathbf{S} = \text{diag}(s_1, \dots, s_K)$, where $s_l = \text{sign}(\langle \hat{\psi}_l, \psi_l \rangle)$. The VAR process can be written as $\mathbf{S} \mathbf{F}_t^* = \sum_{i=1}^p \tilde{\mathbf{A}}_i \mathbf{S} \mathbf{F}_{t-i}^* + \mathbf{S} \eta_t$ since $\mathbf{S} \mathbf{S} = \mathbf{I}_K$, and the aligned sign-adjusted stacked population coefficient matrix is

$$\mathbf{A}^* = \begin{cases} [\mathbf{R}'_{K,J} \tilde{\mathbf{A}}_1 \mathbf{R}_{K,J}, \dots, \mathbf{R}'_{K,J} \tilde{\mathbf{A}}_p \mathbf{R}_{K,J}, \mathbf{0}_{J^*,(m-p)J^*}], & \text{if } m > p, \\ [\mathbf{R}'_{K,J} \tilde{\mathbf{A}}_1 \mathbf{R}_{K,J}, \dots, \mathbf{R}'_{K,J} \tilde{\mathbf{A}}_p \mathbf{R}_{K,J}], & \text{if } m \leq p. \end{cases}$$

Theorem 2. *Let Assumptions 1–3 hold true, and let p_{\max} and K_{\max} be bounded integers such that $p_{\max} \geq p$, $K_{\max} \geq K$. Furthermore, for any t , the covariance operator of \mathbf{Y}_t has infinitely many positive eigenvalues. Then, for any selected numbers of lags $m \leq p_{\max}$ and factors $J \leq K_{\max}$, as $T \rightarrow \infty$:*

- (a) *If $J \geq K$ and $m \geq p$, $\|\hat{\mathbf{A}}^* - \mathbf{A}^*\|_M = O_p(T^{-1/2})$;*
- (b) *If $J < K$, $m < p$, or both, $\text{plim}_{T \rightarrow \infty} \|\hat{\mathbf{A}}^* - \mathbf{A}^*\|_M > 0$.*

Theorem 2 shows that the consistency of the LS estimator hinges on the condition that $J \geq K$ and $m \geq p$. If either J or m is smaller than the actual values, the vector

autoregression cannot be consistently estimated using the conditional LS estimator. This underscores the importance of the simultaneous selection of K and p when employing the LS estimator. For example, if the selected number of factors exceeds K and the chosen lags are $m < p$, the LS estimator is biased. However, it is consistent when $m \geq p$.

The central insight from Theorem 2 is that the MSE is asymptotically minimized when $J \geq K$ and $m \geq p$. Specifically, a model estimated with $K + j$ factors and $p + i$ lags for $i, j > 0$ cannot asymptotically fit worse than a model with K factors and p lags. Once the threshold with the true K and p is met, an increase in the number of selected factors and lags does not impact the asymptotic MSE, but it may lead to parameter proliferation and a loss of efficiency. Consequently, we propose an MSE-based information criterion for estimating K and p of the form

$$\text{CR}_T(J, m) = f(\text{MSE}_T(J, m)) + g_T(J, m), \quad (9)$$

where $g_T(J, m)$ serves as a penalty term for overfitting the model, and $f(\cdot)$ is a strictly increasing function. Then, the numbers of factors and lags are estimated as

$$(\hat{K}, \hat{p}) = \underset{\substack{J=1, \dots, K_{\max} \\ m=1, \dots, p_{\max}}}{\text{argmin}} \text{CR}_T(J, m).$$

Theorem 3. *Let the conditions of Theorem 2 hold true. Let $g_T(J, m)$ be strictly monotonically increasing in both arguments J and m such that $g_T(J, m) \rightarrow 0$ and $Tg_T(J, m) \rightarrow \infty$ for all $0 \leq J \leq K_{\max}$ and $0 \leq m \leq p_{\max}$, as $T \rightarrow \infty$. Then,*

$$\lim_{T \rightarrow \infty} \text{P}(\hat{K} = K, \hat{p} = p) = 1.$$

The results of Theorem 3 indicate that penalized MSE-based information criteria select both the correct number of factors and lags with probability 1. The crucial element for the consistent estimation of K and p is a penalty term that vanishes at an appropriate rate to ensure that an overparameterized model is not chosen. Commonly employed penalty

terms from established information criteria in multivariate time series analysis, such as the Bayesian Information Criterion (BIC) and the Hannan-Quinn Criterion (HQC), meet the conditions outlined in Theorem 3. Furthermore, it is also standard practice to use a logarithmic transformation to put all terms of the generic information criterion (9) onto the same scale. These practical considerations naturally lead us to propose two types of information criteria for estimating K and p . First, a BIC-type estimator is formulated as

$$(\hat{K}_{\text{bic}}, \hat{p}_{\text{bic}}) = \underset{\substack{L=1, \dots, K_{\max} \\ m=1, \dots, p_{\max}}}{\operatorname{argmin}} \log(MSE_T(J, m)) + Jm \frac{\log(T)}{T}, \quad (10)$$

where Jm is the number of estimated parameters in the model, and $T^{-1} \log(T)$ is the penalization rate. Second, the HQC-type estimator employs a lower penalization rate and is formulated as

$$(\hat{K}_{\text{hqc}}, \hat{p}_{\text{hqc}}) = \underset{\substack{L=1, \dots, K_{\max} \\ m=1, \dots, p_{\max}}}{\operatorname{argmin}} \log(MSE_T(J, m)) + 2Jm \frac{\log(\log(T))}{T}. \quad (11)$$

Both (10) and (11) satisfy the conditions from Theorem 3 and are therefore provide consistent estimators for K and p . In practice, the minimization problem can be solved by grid search, where K_{\max} and p_{\max} must be selected.

3.3 Practical guidance

This section details the practical implementation of our estimation method and information criterion. Our primary objective is to present a procedure that can be easily executed using existing software. Building upon the theoretical foundations established in Section 3, we offer two approaches for implementing the information criterion: one based on the analytical representation of the expression in (9), and the other based on a graphical representation. Both methods require numerical integration for computing empirical eigenfunctions and eigenvalues. Additionally, we provide an estimation and prediction algorithm that outlines how one can execute an empirical analysis of a factor

models of functional time series. Our accompanying R package facilitates the execution of all proposed steps.

Analytical representation. Given the selected number of factors J and lags m , the fitted factor and error components are

$$\widehat{\chi}_t^{(J)}(r) = \widehat{\mu}(r) + \sum_{l=1}^J \widehat{F}_{l,t} \widehat{\psi}_l(r), \quad \widehat{\epsilon}_t^{(J)}(r) = Y_t(r) - \widehat{\chi}_t^{(J)}(r),$$

where $Y_t(r) = \widehat{\chi}_t^{(J)}(r) + \widehat{\epsilon}_t^{(J)}(r)$. The one-step ahead curve predictor can be written as $\widehat{Y}_{t|t-1}^{(J,m)}(r) = \widehat{\mu}(r) + \sum_{l=1}^J \widehat{F}_{l,t|t-1} \widehat{\psi}_l(r)$ with $\widehat{F}_{t|t-1}^{(J)} = (\widehat{F}_{1,t|t-1}, \dots, \widehat{F}_{J,t|t-1})' = \widehat{\mathbf{A}}_{(J,m)} \widehat{\mathbf{x}}_{t-1}^{(J,m)}$, and the functional forecast error is

$$Y_t(r) - \widehat{Y}_{t|t-1}^{(J,m)}(r) = \sum_{l=1}^J \widehat{\eta}_{l,t} \widehat{\psi}_l(r) + \widehat{\epsilon}_t^{(J)}(r),$$

where $\widehat{\eta}_{l,t} = \widehat{F}_{l,t} - \widehat{F}_{l,t|t-1}$ are the VAR residuals. From the orthonormality of the estimated loading functions, the MSE given in (8) simplifies to

$$\begin{aligned} MSE_T(J, m) &= \frac{1}{T-m} \sum_{t=m+1}^T \left(\sum_{l=1}^J \widehat{\eta}_{l,t}^2 + \|\widehat{\epsilon}_t^{(J)}\|^2 \right) \\ &\approx \text{tr}(\widehat{\Sigma}_\eta^{(J,m)}) + \int_a^b \frac{1}{T} \sum_{t=1}^T (\widehat{\epsilon}_t^{(J)}(r))^2 dr. \end{aligned} \quad (12)$$

The advantage of the expression (12) over the MSE in (8) is that all components can be easily computed. In particular, $\widehat{\Sigma}_\eta^{(J,m)}$ is the least squares estimator of Σ_η obtained by fitting a VAR(m) model based on the J -variate time series $\widehat{F}_t^{(J)}$. The integral residual sample variance $\int_a^b \frac{1}{T} \sum_{t=1}^T (\widehat{\epsilon}_t^{(J)}(r))^2 dr$ equals the sum of all eigenvalues of the sample covariance operator of the residual curves $\widehat{\epsilon}_t^{(J)}$.

Graphical representation. A careful inspection of the proof of Theorem 3 shows that the MSE reaches its asymptotic minimum when $J \geq K$ and $m \geq p$. This result can be used to select (K, p) graphically, similar to the concept of the scree plot. More precisely,

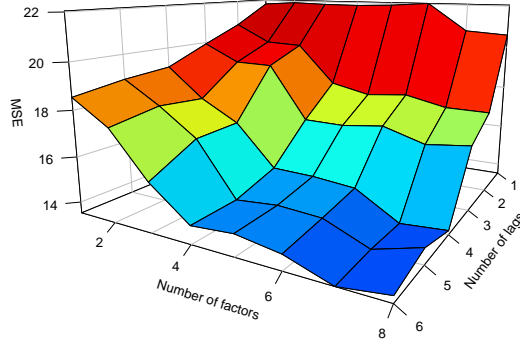


Figure 1: Graphical representation of the MSE using simulated data ($K = p = 4$)

one can plot $MSE_T(J, m)$ for various combinations of J and m and choose the minimum vertex of a rectangular surface with respect to J and m for which the MSE remains “flat”. For this purpose, expression (12) can be used. Figure 1 shows an example illustrating an MSE surface. This figure suggests that $\hat{K} = 4$ and $\hat{p} = 4$ should be selected.

The graphical approach has an advantage over the analytical expressions presented in (10) and (11), since it does not require the specification of the penalty term. However, it cannot be automated when it comes to multiple model selection (for instance, in Monte Carlo simulations). Furthermore, it often comes to a subjective decision of a researcher where the smallest point of the MSE rectangular “flat” area is since the estimated MSE will also fluctuate in this area in finite samples.

Estimation and prediction algorithm.

Step 1: Estimation of parameter functions. Compute the sample mean function $\hat{\mu}(r)$ and the cumulative autocovariance function $\hat{d}(r, s)$ from the observed curves $Y_1(r), \dots, Y_T(r)$. Fix K_{max} large enough and compute eigencomponents $\{(\hat{\lambda}_l, \hat{\psi}_l)\}_{l=1}^{K_{max}}$ and sample scores $\hat{F}_{l,t} = \langle Y_t - \hat{\mu}, \hat{\psi}_l \rangle$, $l = 1, \dots, K_{max}$ as estimates for the factors.

Step 2: Estimation of K , p , and the factor dynamics. Fix p_{max} large enough, compute $MSE_T(J, m)$ from (12) for $J = 0, \dots, K_{max}$ and $m = 0, \dots, p_{max}$, and select K and p according to the BIC or HQC criterion in (10)–(11). Estimate a $\text{VAR}(\hat{p})$ model by the LS estimator given in (7), yielding $[\hat{A}_1^{(\hat{K})}, \dots, \hat{A}_p^{(\hat{K})}] = \hat{\mathbf{A}}_{(\hat{K}, \hat{p})}$.

Step 3: Fitted curves and forecasting. Compute the fitted curves for $t = 1, \dots, T$ as follows: $\hat{Y}_t(r) = \hat{\mu}(r) + \sum_{l=1}^{\hat{K}} \hat{F}_{l,t} \hat{\psi}_l(r)$. Compute the $\text{VAR}(\hat{p})$ factor forecasts as $\hat{F}_{T+1|T}^{(\hat{K})} =$

$\sum_{i=1}^{\hat{p}} \hat{A}_i^{(\hat{K})} \hat{F}_{T+1-i|T}^{(\hat{K})}$ with $\hat{F}_{T+j|T}^{(\hat{K})} = \hat{F}_{T+j}^{(\hat{K})}$ for $j \leq 0$. The h -step curve forecast is given by $\hat{Y}_{T+h|T}^{(\hat{K}, \hat{p})}(r) = \hat{\mu}(r) + (\hat{\Psi}^{(\hat{K})}(r))' \hat{F}_{T+h|T}^{(\hat{K})}$.

4 Simulations

We evaluate the finite sample properties of our estimators through Monte Carlo simulations. Functional time series are generated in the space spanned by the first 20 Fourier basis functions, given as $v_1(r) = 1$, $v_{2j}(r) = \sqrt{2} \sin(2j\pi r)$, and $v_{2j+1}(r) = \sqrt{2} \cos(2j\pi r)$ for $j = 1, \dots, 20$. We use a subset \mathcal{I} of these Fourier functions to specify the loading functions as $(\psi_1, \dots, \psi_K) = (v_j, j \in \mathcal{I})$, while the remaining functions are used to form the error component. This leads to the following data generating procedure:

$$Y_t(r) = \sum_{l=1}^K F_{l,t} \psi_l(r) + \sum_{j \in \mathcal{I}^c} e_{j,t} v_j(r), \quad (13)$$

where $\mathcal{I}^c = \{1, \dots, 20\} \setminus \mathcal{I}$. Here, the first term represents the factor component (2), while the second term represents the error component. Their stochastic nature is generated through a random score vector $e_t = (e_{1,t}, \dots, e_{20,t})' \sim \mathcal{N}(0, \text{diag}(1, 2^{-1}, \dots, 20^{-1}))$, which is independent across $t = 1, \dots, T$. The elements with indices \mathcal{I}^c of this vector are used to form the error term, as given in (13), and the factors are defined as follows:

$$F_t = (F_{1,t}, \dots, F_{K,t})' = A(L)\eta_t, \quad \eta_t' = (\eta_{1,t}, \dots, \eta_{K,t}) = (e_{j,t}, j \in \mathcal{I}).$$

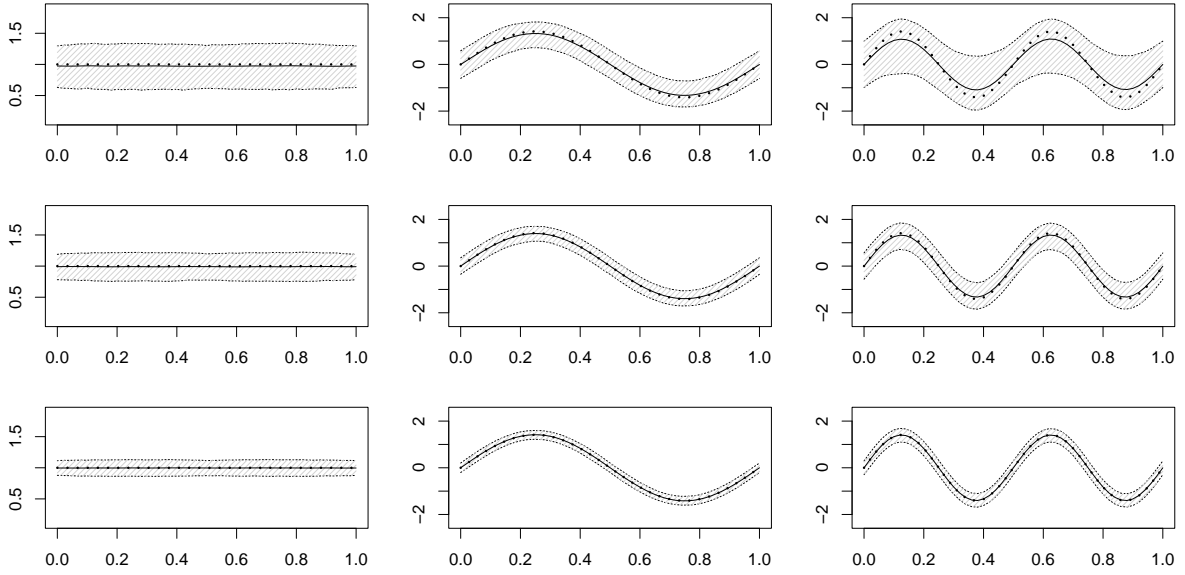
We consider five scenarios, M1–M5, for the dynamics of the factors, represented by $A(L)$, and subsets \mathcal{I} of Fourier basis functions that form the factor space and indicate the number of the factors, detailed in Table 1. It is noteworthy that the scenarios we investigate encompass empirically relevant and challenging cases where the error component can have a higher variance compared to the factors. The single-factor models M1–M3 have different loading functions and factor variances, model M4 uses a two-factor setup, and M5 is similar to the three-factor setup used in Aue et al. (2015). Figure 2 and Table 2

Table 1: Model specifications for the Monte Carlo simulations

Model	K	$H_F = \text{span}(v_l, l \in \mathcal{I})$	p	Lag polynomial $A(L)$
M1	1	$\mathcal{I} = \{1\}$	2	$1 - 0.4L - 0.4L^2$
M2	1	$\mathcal{I} = \{2\}$	2	$1 - 0.4L - 0.4L^2$
M3	1	$\mathcal{I} = \{4\}$	2	$1 - 0.4L - 0.4L^2$
M4	2	$\mathcal{I} = \{2, 3\}$	3	$\mathbf{I}_2 - \begin{pmatrix} 0.6 & -0.2 \\ 0.0 & 0.2 \end{pmatrix} L - \begin{pmatrix} -0.25 & -0.1 \\ 0.00 & -0.1 \end{pmatrix} L^2 - \begin{pmatrix} 0.6 & -0.25 \\ 0.0 & 0.85 \end{pmatrix} L^3$
M5	3	$\mathcal{I} = \{3, 4, 5\}$	1	$\mathbf{I}_3 - \begin{pmatrix} -0.05 & -0.23 & 0.76 \\ 0.80 & -0.05 & 0.04 \\ 0.04 & 0.76 & 0.23 \end{pmatrix} L$

Note: This table outlines the specifications for model (13) used in the results for Table 2 and Figure 2.

Figure 2: Estimation uncertainty of $\hat{\psi}_1$ in models M1–M3



Note: This panel shows the estimation uncertainty of the sign corrected estimator $s_1 \hat{\psi}_1$ based on 10,000 Monte Carlo replications using $q_0 = 1$ for models M1–M3 from Table 1, organized by column, and different sample sizes $T = 100, 200, 500$, organized by row. Each plot includes a dotted line indicating the true value of ψ_1 , a solid line for the sample mean curve of all estimates, and dashed lines marking the pointwise 5% and 95% sample quantiles of the estimates.

confirm our theoretical findings and illustrate the consistency of $\hat{\psi}_l$ as well as the BIC-type and HQ-type information criteria from equations (10) and (11). The estimators \hat{K}_{bic} , \hat{p}_{bic} , \hat{K}_{hqc} , and \hat{p}_{hqc} provide a good approximation of the true parameters for reasonable sample sizes.

Table 2: Finite sample performances of models M1–M5

Model	$\widehat{\chi}$ -err	RMSE				Bias				% of false selection			
		\widehat{K}_{bic}	\widehat{K}_{hqc}	\widehat{p}_{bic}	\widehat{p}_{hqc}	\widehat{K}_{bic}	\widehat{K}_{hqc}	\widehat{p}_{bic}	\widehat{p}_{hqc}	\widehat{K}_{bic}	\widehat{K}_{hqc}	\widehat{p}_{bic}	\widehat{p}_{hqc}
M1													
$T = 100$	0.10	0.02	0.06	0.80	0.62	0.00	0.00	0.64	0.38	0.00	0.00	0.64	0.39
$T = 200$	0.04	0.01	0.02	0.37	0.18	0.00	0.00	0.13	0.03	0.00	0.00	0.13	0.03
$T = 500$	0.01	0.00	0.00	0.00	0.03	0.00	0.00	0.00	0.00	0.00	0.00	0.00	0.00
M2													
$T = 100$	0.18	0.09	0.20	0.98	0.91	-0.01	-0.04	0.96	0.84	0.01	0.03	0.96	0.84
$T = 200$	0.06	0.03	0.08	0.85	0.57	0.00	-0.01	0.72	0.32	0.00	0.01	0.72	0.32
$T = 500$	0.02	0.00	0.01	0.12	0.03	0.00	0.00	0.02	0.00	0.00	0.00	0.02	0.00
M3													
$T = 100$	0.39	0.17	0.36	1.00	0.99	-0.03	-0.12	1.00	0.99	0.03	0.11	1.00	0.99
$T = 200$	0.14	0.14	0.27	1.00	0.94	-0.02	-0.07	0.99	0.88	0.02	0.07	0.99	0.88
$T = 500$	0.03	0.03	0.08	0.77	0.28	0.00	-0.01	0.59	0.08	0.00	0.01	0.59	0.08
M4													
$T = 100$	1.00	0.88	0.81	1.64	1.07	0.77	0.42	1.35	0.56	0.78	0.62	0.68	0.29
$T = 200$	0.51	0.59	0.81	0.47	0.07	0.14	-0.32	0.11	0.00	0.32	0.37	0.06	0.00
$T = 500$	0.22	0.46	0.73	0.00	0.00	-0.15	-0.32	0.00	0.00	0.12	0.23	0.00	0.00
M5													
$T = 100$	0.30	0.31	0.46	0.00	0.00	0.02	-0.16	0.00	0.00	0.09	0.17	0.00	0.00
$T = 200$	0.13	0.12	0.34	0.00	0.00	-0.01	-0.11	0.00	0.00	0.02	0.10	0.00	0.00
$T = 500$	0.05	0.08	0.30	0.00	0.00	-0.01	-0.08	0.00	0.00	0.01	0.08	0.00	0.00

Note: The simulation results are derived using different sample sizes T across models M1–M5 (Table 1), with 10,000 Monte Carlo replications. The first column shows the average estimation error $\|\widehat{\chi}_t - \chi_t\|$ over all observations and replications, where the BIC estimator for K is used to compute $\widehat{\chi}_t$. Subsequent columns report biases, root mean square errors (RMSE), and frequencies of false selection for the BIC and HQC estimators from equations (10) and (11), using $q_0 = 1$, and $Kmax = 8$ and $p_{max} = 8$ for the maximum number of factors and lags, respectively.

5 Empirical applications

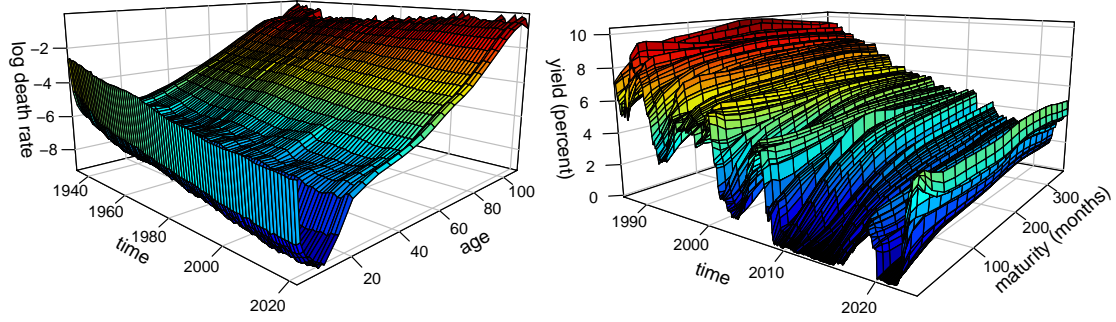
We apply our methodology to two datasets that naturally align with a functional time series perspective: yearly mortality rate curves and monthly bond yield curves (see Figure 3). The first dataset consists U.S. log mortality rate curves of the male population, defined as $Y_t(r) = \log(D_t(r)/P_t(r))$, where $D_t(r)$ represents the number of deaths in calendar year t for individuals aged r , and $P_t(r)$ denotes the corresponding population of age r . This dataset is available from the Human Mortality Database², comprising $T = 90$ yearly curves, each observed at 111 equidistant points spanning ages 0 to 110.

The second dataset, from Liu and Wu (2021)³, consists of reconstructed annualized continuously-compounded zero-coupon U.S. Treasury yield curves. Each curve is given by $Y_t(r)$, where t denotes the calendar month and r the time to maturity in months. The dataset spans November 1985 to December 2023 ($T = 458$), with each curve containing

²Accessible via the R package `demography`, though website registration at <https://www.mortality.org> is required.

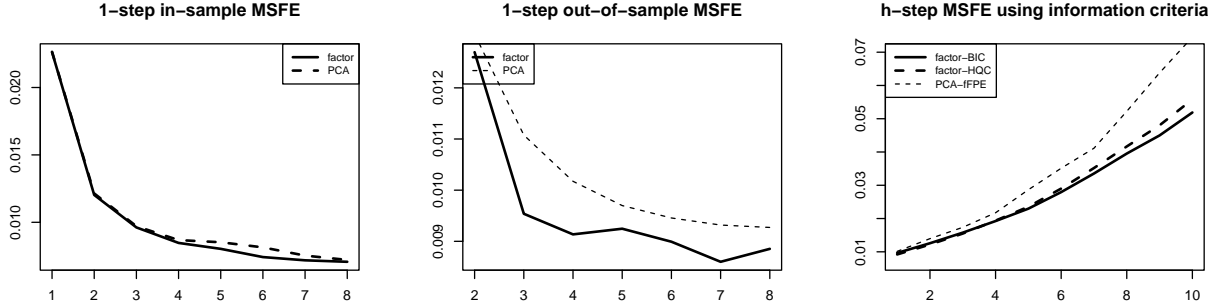
³Data source: <https://sites.google.com/view/jingcynthiawu/yield-data>.

Figure 3: Log mortality rate curves for U.S. males and U.S. Treasury yield curves



Note: The figure depicts the two functional time series datasets used in the empirical applications.

Figure 4: VAR(1) forecasting results for the mortality data



Note: The three panels show: (left) in-sample MSEs for factor-based ($q_0 = 1$) and PCA-based VAR(1) predictions across number of selected components; (middle) out-of-sample rolling MSFEs with VAR(1) across number of selected components; (right) h -step rolling out-of-sample MSFEs using rolling selected components and lags across forecast horizon h .

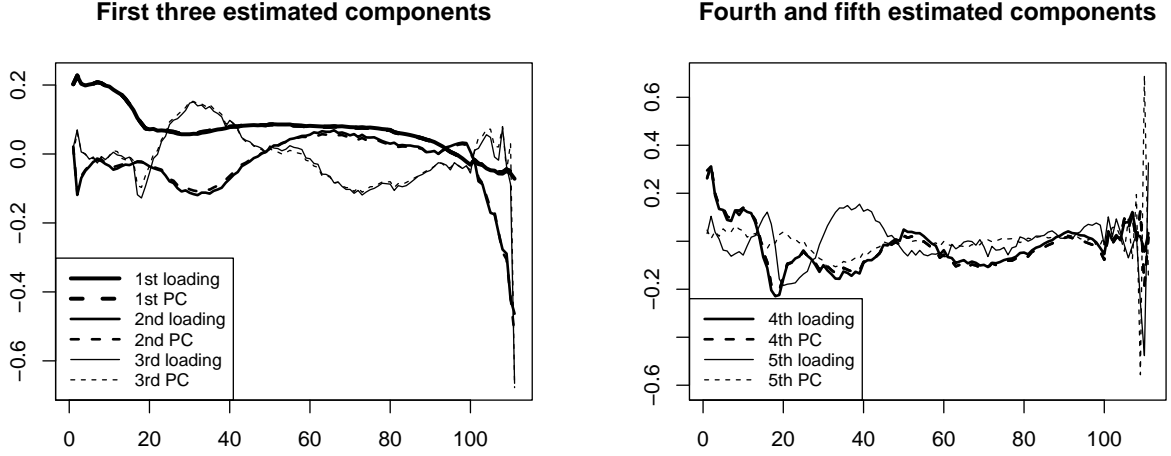
360 equidistant observations corresponding to maturities from 1 to 360 months.

5.1 Mortality curve forecasting

Mortality rates, when viewed across age groups over time, naturally take the form of functional curves, making them well-suited for functional time series analysis. U.S. mortality rate curves have been widely used in the literature, including in [Kokoszka and Reimherr 2017](#), to illustrate functional PCA-based forecasting methods developed in [Hyndman and Ullah \(2007\)](#) and [Aue et al. \(2015\)](#). Their approach relies on a truncated Karhunen-Loève expansion:

$$Y_t(r) \approx \hat{\mu}(r) + \sum_{l=1}^J g_{lt} \hat{\phi}_l(r), \quad g_{lt} = \langle Y_t - \hat{\mu}, \hat{\phi}_l \rangle,$$

Figure 5: Factor loadings and principal components for the mortality data

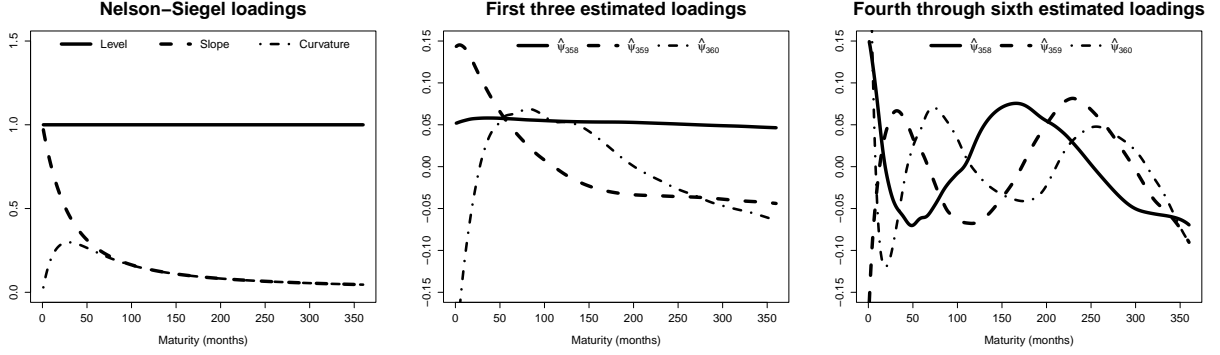


Note: The plots show the first five estimated factor loadings and functional principal components (PC).

where $\hat{\phi}_l$ are the sample functional principal components of Y_1, \dots, Y_T . The forecasted curve is $\hat{\mu}(r) + \sum_{l=1}^J \hat{g}_{l,T+h|T} \hat{\phi}_l(r)$, where $\hat{g}_{l,T+h|T}$ are predicted scores obtained from a multivariate time series model for the vectors of sample functional principal component scores $(\hat{g}_{1t}, \dots, \hat{g}_{Jt})'$. To determine the optimal truncation parameter J , [Aue et al. \(2015\)](#) propose a functional final prediction error (fFPE) information criterion. While this approach is widely used and serves as a proven forecasting method, its key limitation is that the first J functional principal components do not necessarily align with the most predictable components of the functional time series.

Using the full sample, we obtain $\hat{K}_{\text{bic}} = 6$, $\hat{K}_{\text{hqc}} = 7$, and $\hat{p}_{\text{bic}} = \hat{p}_{\text{hqc}} = 1$, while the fFPE criterion suggests using $J = 8$ functional principal component scores with one lag. The in-sample mean squared forecast errors (MSFE) for $\hat{K}_{\text{hqc}} = 7$ factors is lower than for $J = 8$ principal components (as suggested by the fFPE criterion), which indicates that our approximate functional factor model provides a more parsimonious dynamic representation than the PCA-based approach. Furthermore, the left panel of [Figure 4](#) confirms that factor-based predictions yield uniformly lower in-sample MSFE than PCA-based predictions for the same number of included components ranging from 1 to 8. The difference becomes noticeable when higher-order components are included. This is because the first three factor loadings closely resemble the first three functional principal

Figure 6: Loading functions of the DNS model and yield curve data

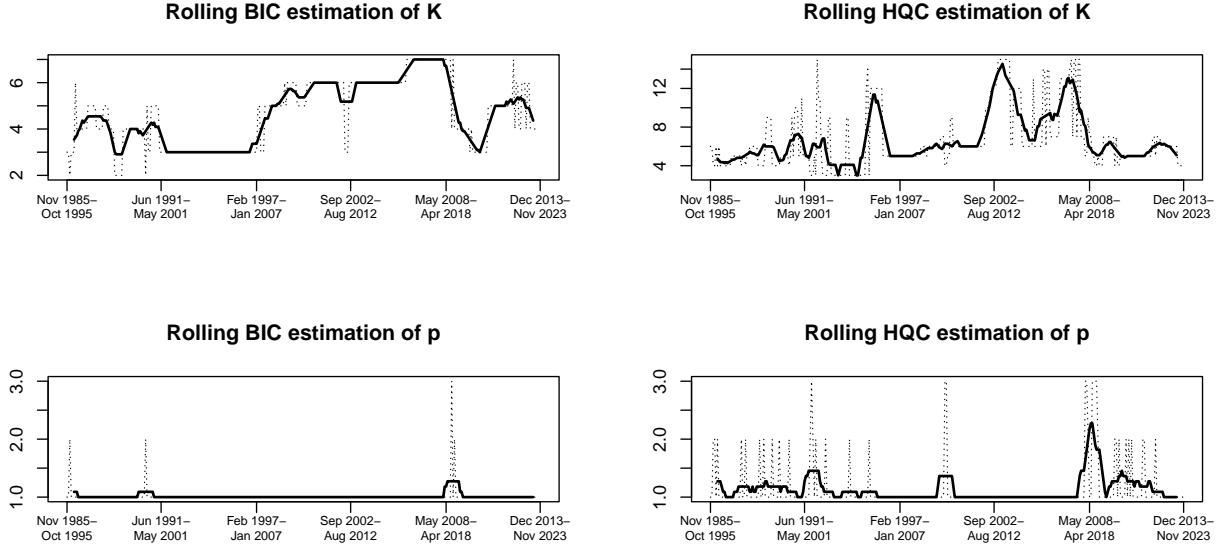


Note: The figure displays the three standard loading functions from the dynamic Nelson-Siegel model fom (14) (left), the first three estimated loading functions from our functional factor model (middle), and the fourth through sixth estimated loading functions (right).

components, whereas the fourth and fifth factor loadings deviate significantly from the PCA counterparts (see Figure 5).

This difference becomes more prominent when we evaluate out-of-sample forecasts using a rolling window approach with a window size of 50 observations. Model parameters are estimated within the rolling training sample, and h -step out-of-sample MSFEs are computed. The second plot of Figure 4 shows that factor-based predictions more clearly outperform PCA-based predictions for 1-step forecasts in the VAR(1) model when ranging the number of included factors from 1 to 8. Furthermore, when turning to h -step ahead forecasts where $h = 1, \dots, 10$, we find another argument why structural representation of the dynamics is important. The right panel of Figure 4 demonstrates that factor-based predictions using a VAR(p) model with K factors, where K and p are selected via the BIC or HQC criterion, increasingly outperform forecasts from a VAR(p) model with J functional principal component scores, where J and p are chosen using the fFPE criterion of Aue et al. (2015) with increasing h . In conclusion, by focusing on factors that capture the underlying dynamics of the process, we obtain better forecasting performance compared to the traditional PCA-based approach.

Figure 7: Rolling estimation of K and p for the yield curve data



Note: The figure shows rolling window estimates (120 months) of the number of factors K (top) and lags p (bottom) over time, selected by BIC and HQC criteria. The dotted lines show the actual estimates while the solid lines indicate the simple two-sided moving average filter of order 11.

5.2 Yield curve modeling

The dynamic Nelson-Siegel (DNS) framework introduced first by [Nelson and Siegel \(1987\)](#) and further developed by [Diebold and Li \(2006\)](#) has emerged as a workhorse model in the financial econometrics literature and has been the basis for many modifications and extensions (see [Svensson 1995](#), [Christensen et al. 2009](#), [Lengwiler and Lenz 2010](#), and [Diebold and Rudebusch 2013](#)). Functional factor models also find their role in the analysis of the term structure of bond yields. For instance, functional data models for yield curves have been explored (see [Hays et al. 2012](#), [Bardsley et al. 2017](#), [Sen and Klüppelberg 2019](#), and [Horváth et al. 2022](#)).

Central to the models of the Nelson-Siegel class is the assumption that the bond yield $Y_t(r)$ with time to maturity $r \in [a, b]$ at point in time t follows a strict factor model framework that incorporates an additive discrete white noise component. The curve process is represented as $Y_t(r_i) = \tilde{\chi}_t(r_i) + \tilde{\epsilon}_{i,t}$, where $\tilde{\chi}_t$ denotes a finite-dimensional factor component, $\tilde{\epsilon}_{i,t}$ is white noise across i and t , and r_1, \dots, r_N forms the discrete grid of available maturities. The shape of the loading functions and the number of factors are treated as pre-specified parameters. Specifically, the DNS model assumes the three-factor

Table 3: Rolling out-of-sample MSFEs for the yield curve data

horizon	maturity	BIC OLS	HQC OLS	PCA OLS	BIC lasso	HQC lasso	PCA lasso	DNS p=1	DNS p=2
rolling window: 120 months									
1-step	short	0.918	0.903	1.332	0.983	0.994	1.103	1.701	1.710
	medium	1.213	1.185	1.748	1.215	1.208	1.206	1.758	1.672
	long	1.159	1.190	1.836	1.120	1.157	1.181	1.327	1.375
3-step	short	0.915	0.936	1.317	0.882	0.876	0.946	1.113	1.076
	medium	1.255	1.260	1.671	1.039	1.010	1.035	1.337	1.284
	long	1.362	1.416	1.872	1.027	1.031	1.049	1.265	1.359
6-step	short	1.120	1.127	1.569	0.887	0.899	0.934	1.067	1.077
	medium	1.470	1.485	2.009	0.997	0.978	0.988	1.284	1.295
	long	1.615	1.691	2.337	0.992	0.996	1.006	1.296	1.424
12-step	short	2.627	2.626	4.142	0.922	0.928	0.934	1.092	1.086
	medium	3.194	3.219	5.154	0.998	0.975	0.970	1.256	1.248
	long	3.291	3.406	5.433	0.999	0.990	1.001	1.369	1.478
rolling window: 240 months									
1-step	short	0.897	0.858	1.161	0.986	0.939	1.081	1.805	1.803
	medium	1.039	0.945	1.280	0.992	0.934	1.176	2.033	1.833
	long	1.090	1.090	1.373	1.047	1.028	1.102	1.295	1.312
3-step	short	0.803	0.816	0.982	0.915	0.914	0.923	1.038	0.939
	medium	1.000	1.022	1.220	0.951	0.942	1.008	1.302	1.156
	long	1.178	1.195	1.393	0.988	0.989	1.020	1.158	1.179
6-step	short	0.797	0.899	1.019	0.922	0.924	0.937	0.936	0.883
	medium	1.028	1.172	1.396	0.957	0.955	0.993	1.156	1.091
	long	1.324	1.403	1.776	0.986	0.989	1.013	1.162	1.211
12-step	short	0.835	0.978	1.173	0.945	0.943	0.944	0.907	0.878
	medium	1.037	1.227	1.665	0.966	0.950	0.970	1.080	1.050
	long	1.430	1.564	2.344	0.991	0.986	0.998	1.183	1.233

Note: The table reports out-of-sample MSFEs relative to the random walk forecast across forecast horizons and maturity segments (short: ≤ 12 months, medium: 12-24 months, long: > 24 months) using 120- and 240-month rolling windows. Bold entries indicate better performance than the random walk benchmark. Forecast methods include functional factor models using BIC/HQC criteria ($q_0 = 1$) with OLS and lasso estimation, PCA-based forecasts with ffPE criterion, and DNS models with VAR(1) and VAR(2) dynamics.

structure

$$\tilde{\chi}_t(r) = F_{1,t} + F_{2,t} \frac{1 - e^{-\xi r}}{\xi r} + F_{3,t} \left(\frac{1 - e^{-\xi r}}{\xi r} - e^{-\xi r} \right) \quad (14)$$

with [Diebold and Li \(2006\)](#) suggesting the decay parameter value $\xi = 0.0609$. The factors, $F_{1,t}, F_{2,t}, F_{3,t}$, are estimated through ordinary least squares at each time t using the available maturities.

[Lengwiler and Lenz \(2010\)](#) and [Nielsen et al. \(2024\)](#) have already highlighted that the

three-factor DNS model fails to fully capture the dynamics of yield curve data, suggesting the need for additional or more complex loading functions. Our information criteria support these findings, estimating the number of factors as $\hat{K}_{\text{bic}} = 5$ and $\hat{K}_{\text{hqc}} = 10$, with the number of lags estimated as $\hat{p}_{\text{bic}} = \hat{p}_{\text{hqc}} = 1$. In Figure 6, we compare the first six estimated loading functions with the pre-specified loadings from the DNS model. The first three estimated loadings show similarities to the DNS loadings in terms of magnitude and curvature and have similar economic interpretations: the first factor represents long-term effects, the second short-term, and the third medium-term. The fourth, fifth and sixth factors mediate between short, long, and medium-term effects.

However, a key finding of our analysis is that the estimated number of factors and lags varies significantly depending on the time period. A rolling window analysis with a 120-month (10-year) window reveals that during periods of economic stability, 3-4 factors suffice, whereas during economic crises, substantially more factors are required. Figure 7 shows that the BIC criterion suggests around four factors until the mid-1990s, a period that includes the 1990–1991 recession and the 1994 bond market crisis. During the relatively stable mid-2000s, the estimated number of factors drops to three. Following the 2007 housing bubble collapse, it increases to seven before fluctuating between three and five in the late 2010s and early 2020s. These findings highlight the sensitivity of factor specifications to prevailing economic conditions. Rather than fixing the number of factors a priori, we strongly recommend that practitioners adopt a data-driven approach to determine the appropriate specification.

To assess the impact of additional factors on forecasting accuracy, we employ a rolling window approach similar to Diebold and Li (2006), performing sequential monthly out-of-sample yield curve forecast comparisons. At each step, we use a fixed rolling window of $w = 120$ and $w = 240$ for the training period. Specifically, the h -step-ahead forecast for time t is based on data from periods $t - h - w$ to $t - h$.

In addition to comparing our forecasts with those from the dynamic DNS model, we include as a benchmark the naive random walk forecast, which is simply the observed curve

of h periods before. [Diebold and Li \(2006\)](#) and [Caldeira et al. \(2025\)](#) previously noted that DNS yield curve forecasts offer little to no improvement over the naive benchmark. Their results suggest that any potential improvements from DNS over the random walk are limited to short- and medium-term interest rates, with no significant gains observed for long-term rates. Therefore, when evaluating the MSFEs, we consider short-term interest rates (up to 12 months to maturity), medium-term interest rates (13 months to 24 months to maturity), and long-term interest rates (25 months to 360 months to maturity) separately.

Table 3 confirms that the DNS model rarely outperforms the random walk forecast. In contrast, functional factor-based forecasts, where K and p are selected using the BIC or HQC criterion, consistently outperform the random walk for short-term interest rate prediction. However, as illustrated in Figure 7, the selected values of K and p can become excessively large in certain periods, leading to overparameterization. Consequently, this can result in suboptimal forecasts, particularly for PCA-based predictions using the ffPE criterion, which often tends to select a large number of components and lags.

To address this issue, we also include forecasts from an L1 shrinkage-estimated VAR model, where K and p are selected based on the HQC criterion. The shrinkage parameter is tuned within each rolling training sample using 10-fold cross-validation, as implemented by default in the `glmnet` R package. Our results indicate that lasso estimators for the factor-based VAR model outperforms all other models, including the random walk, particularly for longer forecasting horizons.

6 Conclusion

This paper provides an in-depth study of the factor model for functional time series, including its identification, estimation, and prediction. From a practical point of view, the approximate functional factor model is an attractive modeling framework for infinitely-dimensional temporal data, as it allows analyses and predictions via a low-dimensional factor component of the data. Our results are useful for a broad range of applications

in which the number of factors is unknown, and the error component potentially has strong cross-correlation and is weakly correlated with the common component. We have developed a simple-to-use novel method, yielding consistent estimates of the number of factors and their dynamics. A Monte Carlo study and an empirical illustration of yield curves show that our method provides an attractive modeling and predictive framework.

Several methodological problems await further analysis. The first is to develop the distributional and inferential theory for the estimators beyond the consistency results obtained in this paper. For instance, in the empirical illustration of yield curves, it might be interesting to provide confidence bands or test some restrictions on the loading functions. The second is to go beyond the weakly stationary assumption on the factors, for instance, by allowing some factors to have short memory while others are permitted to have long memory (persistence). Finally, the third is to develop a predictive methodology for the factors using semiparametric or nonparametric models.

Acknowledgments

We thank Jörg Breitung, Juan Carlos Escanciano, Joachim Freyberger, Tobias Hartl, Justus Henseler, Alois Kneip, Malte Knüppel, Dominik Liebl, Alexander Mayer, Daan Opschoor, and Luis Winter for their valuable comments and suggestions, and Justin Franken for his assistance with software implementations. This work was supported by the Deutsche Forschungsgemeinschaft (DFG) under project number 511905296. Moreover, the first author received financial support from the University of Bonn's Argelander Grants, while the second author was funded by Juan de la Cierva Incorporación, grant number IJC2019-041742-I. Additionally, we acknowledge the use of the CHEOPS HPC cluster for parallel computing.

Supporting Information

An accompanying R package is available at <https://github.com/ottosven/dffm>.

SUPPLEMENTARY MATERIAL TO

Approximate Factor Models for Functional Time Series

by Sven Otto and Nazarii Salish

A Technical Appendix

A.1 Notations and Definitions

In this section, we provide a detailed description of the notations used in this appendix.

Norms

For a function $g \in H = L^2([a, b])$, the squared L^2 norm is $\|g\|^2 = \int_a^b g(r)^2 dr$. The squared Euclidean norm for a vector $\mathbf{a} \in \mathbb{R}^n$ is $\|\mathbf{a}\|_2^2 = \mathbf{a}'\mathbf{a}$, and the squared Frobenius norm for a matrix $\mathbf{A} \in \mathbb{R}^{n \times k}$ with entries A_{ij} is $\|\mathbf{A}\|_M^2 = \sum_{i=1}^n \sum_{j=1}^k A_{ij}^2$. For an integral operator $\mathcal{T} : H \rightarrow H$ with kernel function $\tau(r, s)$, the squared Hilbert-Schmidt norm is $\|\mathcal{T}\|_S^2 = \int_a^b \int_a^b \tau(r, s)^2 ds dr$.

Orthogonalized factor model representation

The transformed factors introduced in Section 2 are defined by the projection coefficients $F_{l,t}^* = \langle Y_t - \mu, \psi_l \rangle$ for $l = 1, \dots, K$ and satisfy the relation $F_{l,t}^* = F_{l,t} + \langle \epsilon_t, \psi_l \rangle$. Assumption 1(c) also holds for the K -variate process $F_t^* = (F_{1,t}^*, \dots, F_{K,t}^*)'$ since the error function is a martingale difference sequence by Assumption 1(a). The factor model has the orthogonalized representation

$$Y_t(r) = (\Psi(r))' F_t^* + \epsilon_t^*(r), \quad (\text{A.1})$$

where the orthogonalized error term defined as

$$\epsilon_t^*(r) := \epsilon_t(r) - \sum_{l=1}^K \langle \epsilon_t, \psi_l \rangle \psi_l(r).$$

Note that ϵ_t^* satisfies $\int_a^b \Psi(r) \epsilon_t^*(r) dr = 0$ for all t , which implies that ϵ_t^* takes values in $H_F^\perp = \text{span}(\psi_1, \dots, \psi_K)^\perp$. Note that $\|\epsilon_t^*\| \leq (K+1)\|\epsilon_t\|$, and Assumptions 1(a) implies that ϵ_t^* is a martingale difference sequence with respect to $\{\epsilon_{t-1}^*, F_{t-1}^*, \epsilon_{t-2}^*, F_{t-2}^*, \dots\}$. Assumption 3 implies that $\sup_{r \in [a, b]} E[(\epsilon_t^*(r))^4] < \infty$, $\sup_{r \in [a, b]} E[(Y_t(r))^4] < \infty$ and $E[(F_{l,t}^*)^4] < \infty$ for any t and $l = 1, \dots, K$.

Sign-adjusted factor model representation

The signs of the loading functions are only identified up to a sign change. Therefore, we condition our notation on the sign transformation matrix $\mathbf{S} = \text{diag}(s_1, \dots, s_K)$, where $s_l = \text{sign}(\langle \widehat{\psi}_l, \psi_l \rangle)$ denotes the selected sign of the l -th sample eigenfunction. The sign-adjusted vectors of loadings and factors are defined as $\widetilde{\Psi}(r) = (\Psi(r))' \mathbf{S}$ and $\widetilde{F}_t = \mathbf{S} F_t^*$, and their l -th components are $\widetilde{\psi}_l = s_l \psi_l$ and $\widetilde{F}_{l,t} = s_l F_{l,t}^*$. Assumptions 1–3 are not affected by the sign-adjustment and also hold for $\widetilde{\Psi}(r)$ and \widetilde{F}_t . Given that $\mathbf{S}\mathbf{S} = \mathbf{I}_K$ and $\widetilde{A}_i = \mathbf{S} A_i \mathbf{S}$, the VAR(p) model of Assumption 3(a) can be written as

$$\widetilde{F}_t = \sum_{i=1}^p \widetilde{A}_i \widetilde{F}_{t-i} + \mathbf{S} \eta_t.$$

To streamline the notation, we define the sign-adjusted stacked coefficient matrix $\widetilde{\mathbf{A}} := [\widetilde{A}_1, \dots, \widetilde{A}_p]$ and the lagged factors vector $\widetilde{\mathbf{x}}_{t-1} := (\widetilde{F}'_{t-1}, \dots, \widetilde{F}'_{t-p})'$. The VAR(p) equation then becomes

$$\widetilde{F}_t = \widetilde{\mathbf{A}} \widetilde{\mathbf{x}}_{t-1} + \mathbf{S} \eta_t.$$

Given that \widetilde{F}_t follows a linear process with innovations $\mathbf{S} \eta_t$ forming a martingale difference sequence, we obtain the normal equation $\widetilde{\Gamma} = \widetilde{\mathbf{A}} \widetilde{\Sigma}$ and the population moment representation

$$\widetilde{\mathbf{A}} = \widetilde{\Gamma} \widetilde{\Sigma}^{-1} = \begin{bmatrix} E[\widetilde{F}_t \widetilde{F}'_{t-1}] & \dots & E[\widetilde{F}_t \widetilde{F}'_{t-p}] \\ \vdots & & \vdots \\ E[\widetilde{F}_{t-p} \widetilde{F}'_{t-1}] & \dots & E[\widetilde{F}_{t-p} \widetilde{F}'_{t-p}] \end{bmatrix}^{-1}.$$

Combining the factor model equation with the newly introduced orthogonalized and sign-adjusted notations, the model has the dynamic representation

$$Y_t(r) = \mu(r) + (\widetilde{\Psi}(r))' \widetilde{F}_t + \epsilon_t^*(r) = \mu(r) + (\widetilde{\Psi}(r))' \widetilde{\mathbf{A}} \widetilde{\mathbf{x}}_{t-1} + (\Psi(r))' \eta_t + \epsilon_t^*(r). \quad (\text{A.2})$$

VAR coefficient matrix estimator

For the selected numbers of factors J and lags m , we define the $J \times 1$ vector of sample scores $\widehat{F}_t^{(J)} = (\widehat{F}_{1,t}, \dots, \widehat{F}_{J,t})'$, where the l -th component is $\widehat{F}_{l,t} = \langle Y_t - \widehat{\mu}, \widehat{\psi}_l \rangle$. The LS estimator can be represented using the stacked vector of lagged sample scores $\widehat{\mathbf{x}}_{t-1}^{(J,m)} = ((\widehat{F}_{t-1}^{(J)})', \dots, (\widehat{F}_{t-m}^{(J)})')'$ and the matrices

$$\widehat{\Gamma}_{(J,m)} = \frac{1}{T} \sum_{t=m+1}^T \widehat{F}_t^{(J)} (\widehat{\mathbf{x}}_{t-1}^{(J,m)})', \quad \widehat{\Sigma}_{(J,m)} = \frac{1}{T} \sum_{t=m+1}^T \widehat{\mathbf{x}}_{t-1}^{(J,m)} (\widehat{\mathbf{x}}_{t-1}^{(J,m)})'.$$

In the scenario of overselection ($J \geq K$ and $m \geq p$), the estimator is

$$\hat{\mathbf{A}}^* = \hat{\mathbf{A}}_{(J,m)} = [\hat{A}_1^{(J)}, \dots, \hat{A}_m^{(J)}] = \hat{\Gamma}_{(J,m)} \hat{\Sigma}_{(J,m)}^{-1}.$$

In cases of lag underselection and factor underselection, we have

$$\hat{\mathbf{A}}^* = \begin{cases} [\mathbf{R}'_{J,K} \hat{A}_1^{(J)} \mathbf{R}_{J,K}, \dots, \mathbf{R}'_{J,K} \hat{A}_m^{(J)} \mathbf{R}_{J,K}, \mathbf{0}_{J^*,(p-m)J^*}] & m < p, \\ [\mathbf{R}'_{J,K} \hat{A}_1^{(J)} \mathbf{R}_{J,K}, \dots, \mathbf{R}'_{J,K} \hat{A}_m^{(J)} \mathbf{R}_{J,K}] & J < K \text{ and } m \geq p, \end{cases}$$

where $J^* = \max\{J, K\}$ and

$$\mathbf{R}_{J,K} = \begin{cases} [\mathbf{I}_J, \mathbf{0}_{J,K-J}], & \text{if } J < K, \\ \mathbf{I}_J, & \text{if } J \geq K. \end{cases}$$

Aligned VAR population coefficients

For the underselection scenarios, the aligned population coefficient matrix is defined as

$$\mathbf{A}^* = \begin{cases} [\mathbf{R}'_{K,J} \tilde{A}_1 \mathbf{R}_{K,J}, \dots, \mathbf{R}'_{K,J} \tilde{A}_p \mathbf{R}_{K,J}] & m < p, \\ [\tilde{A}_1, \dots, \tilde{A}_p, \mathbf{0}_{J,(m-p)J}] & J < K \text{ and } m \geq p. \end{cases}$$

The overselection scenario ($J \geq K$ and $m \geq p$) requires a more complex notation. Our proof of Theorem 2 hinges on the identification of appropriate population counterparts for $\hat{\Gamma}_{(J,m)}$ and $\hat{\Sigma}_{(J,m)}$ that satisfy the equation $\mathbf{A}^* = \tilde{\Gamma}^* (\tilde{\Sigma}^*)^{-1}$. In the special case $J = K$, the aligned matrix is represented as

$$\mathbf{A}^* = \begin{bmatrix} E[\tilde{F}_t \tilde{F}'_{t-1}] & \dots & E[\tilde{F}_t \tilde{F}'_{t-m}] \\ \vdots & & \vdots \\ E[\tilde{F}_{t-m} \tilde{F}'_{t-1}] & \dots & E[\tilde{F}_{t-m} \tilde{F}'_{t-m}] \end{bmatrix}^{-1},$$

where the last $K(m-p)$ columns consist solely of zeros, which follows from the fact that the partial autocorrelation function for a VAR(p) process is zero for lags exceeding p . For the case $J > K$, we introduce the auxiliary block matrices

$$G_{ij} := \begin{cases} \begin{bmatrix} E[\tilde{F}_{t-i} \tilde{F}'_{t-j}] & \mathbf{0}_{K,J-K} \\ \mathbf{0}_{J-K,K} & \mathbf{0}_{J-K,J-K} \end{bmatrix} & \text{for } i \neq j, \\ \begin{bmatrix} E[\tilde{F}_{t-i} \tilde{F}'_{t-i}] & \mathbf{0}_{K,J-K} \\ \mathbf{0}_{J-K,K} & \hat{V}_i \end{bmatrix} & \text{for } i = j, \end{cases}$$

where

$$\widehat{V}_i := \frac{1}{T} \sum_{t=m+1}^T \begin{pmatrix} \widehat{F}_{K+1,t-i} \\ \vdots \\ \widehat{F}_{J,t-i} \end{pmatrix} \begin{pmatrix} \widehat{F}_{K+1,t-i} \\ \vdots \\ \widehat{F}_{J,t-i} \end{pmatrix}'.$$

Since the covariance operator of Y_t has infinitely many positive eigenvalues for any t , the entries of \widehat{V}_i are uniformly bounded away from zero for all $i = 1, \dots, m$. Together with Assumptions 1(b) and 3, it follows that G_{ii} is symmetric and uniformly positive definite. Then, a population counterpart of $\widehat{\Sigma}_{(J,m)}$ can be defined as

$$\widetilde{\Sigma}^* := \begin{bmatrix} G_{11} & \dots & G_{1m} \\ \vdots & & \vdots \\ G_{m1} & \dots & G_{mm} \end{bmatrix},$$

which is symmetric and uniformly positive definite as well.

Notice that, for the column and row indices $(j_1, j_2) \in \mathcal{I}_i = \{(i-1)J+K+1, \dots, iJ\}$, the entries of $\widehat{\Sigma}_{(J,m)}$ and $\widetilde{\Sigma}^*$ coincide for all $i = 1, \dots, m$ because \widehat{V}_i are also the corresponding block entries of $\widehat{\Sigma}_{(J,m)}$. This is a convenient notation because the corresponding block diagonal entries of the difference $\widehat{\Sigma}_{(J,m)} - \widetilde{\Sigma}^*$ are zero by definition. Moreover, focusing on the column and row indices from the set \mathcal{I}_i for $i = 1, \dots, m$, the inverse $(\widetilde{\Sigma}^*)^{-1}$ has the same block structure as $\widetilde{\Sigma}^*$ with

$$(\widetilde{\Sigma}^*)^{-1} = \begin{bmatrix} * & \mathbf{0} & * \\ \mathbf{0} & \widehat{V}_i & \mathbf{0} \\ * & \mathbf{0} & * \end{bmatrix}^{-1} = \begin{bmatrix} * & \mathbf{0} & * \\ \mathbf{0} & \widehat{V}_i^{-1} & \mathbf{0} \\ * & \mathbf{0} & * \end{bmatrix},$$

where the entries of the diagonal blocks \widehat{V}_i do not affect any other entry of the inverse of that matrix (see, e.g., Lütkepohl 1996 Section 3.5.3). We define the population equivalent of $\widehat{\Gamma}_{(J,m)}$ as

$$\widetilde{\Gamma}^* := \begin{bmatrix} G_{01} & \dots & G_{0m} \end{bmatrix},$$

which is a $J \times Jm$ matrix consisting of zeros at the columns with indices from the index set $\mathcal{I} = \cup_{i=1}^m \mathcal{I}_i$. Consequently, the entries of the product $\widetilde{\Gamma}^*(\widetilde{\Sigma}^*)^{-1}$ do not depend on \widehat{V}_i and are zero for the column and row indices $(j_1, j_2) \in \mathcal{I}_i$ for all $i = 1, \dots, m$. Therefore,

$$\mathbf{A}^* = \widetilde{\Gamma}^*(\widetilde{\Sigma}^*)^{-1} = \begin{bmatrix} G_{01} & \dots & G_{0m} \end{bmatrix} \begin{bmatrix} G_{11} & \dots & G_{1m} \\ \vdots & & \vdots \\ G_{m1} & \dots & G_{mm} \end{bmatrix}^{-1}.$$

Aligned one-step ahead curve predictor

The estimated one-step ahead curve predictor can be written as

$$\hat{Y}_{t|t-1}^{(J,m)}(r) = \hat{\mu}(r) + (\hat{\Psi}^{(J)}(r))' \hat{\mathbf{A}}_{(J,m)} \hat{\mathbf{x}}_{t-1}^{(J,m)} = \hat{\mu}(r) + (\hat{\Psi}^{(J^*)}(r))' \hat{\mathbf{A}}^* \hat{\mathbf{x}}_{t-1}^{(J^*,m^*)}, \quad (\text{A.3})$$

where $J^* = \max\{J, K\}$ and $m^* = \max\{m, p\}$, and its population counterpart is

$$\tilde{Y}_{t|t-1}(r) = \mu(r) + (\tilde{\Psi}(r))' \tilde{\mathbf{A}} \tilde{\mathbf{x}}_{t-1} = \mu(r) + (\tilde{\Psi}^{(J^*)}(r))' \mathbf{A}^* \tilde{\mathbf{x}}_{t-1}^{(J^*,m^*)}, \quad (\text{A.4})$$

where we set $\tilde{\Psi}^{(J^*)}(r) = \tilde{\Psi}(r)$ for $J \leq K$, and $\tilde{\Psi}^{(J^*)}(r) = ((\tilde{\Psi}(r))', \mathbf{0}_{J-K}')'$ for $J > K$.

A.2 Proof of Proposition 1

Since (λ_l, ψ_l) are the eigencomponents of D , we have

$$\begin{aligned} & \lim_{T \rightarrow \infty} \sum_{\tau=1}^{q_0} \int_a^b \left(\frac{1}{T} \sum_{t=\tau+1}^T \text{Cov}[\langle Y_t - \mu, \psi_l \rangle, Y_{t-\tau}(q)] \right)^2 dq \\ &= \int_a^b \int_a^b \sum_{\tau=1}^{q_0} \int_a^b c_\tau(r, q) c_\tau(s, q) \psi_l(s) \psi_l(r) ds dr dq \\ &= \int_a^b \int_a^b d(r, s) \psi_l(s) \psi_l(r) ds dr = \lambda_l. \end{aligned}$$

Furthermore, we have $\sum_{j=1}^K \langle \psi_j, f \rangle^2 \leq \|gf\| = 1$ and $\sum_{j=1}^{l-1} \langle \psi_j, f \rangle^2 = 0$ because $f \in \text{span}(\psi_1, \dots, \psi_{l-1})^\perp$. Recall that $d(r, s) = \sum_{l=1}^K \lambda_l \psi_l(r) \psi_l(s)$. Then,

$$\begin{aligned} & \lim_{T \rightarrow \infty} \sum_{\tau=1}^{q_0} \int_a^b \left(\frac{1}{T} \sum_{t=\tau+1}^T \text{Cov}[\langle Y_t - \mu, f \rangle, Y_{t-\tau}(q)] \right)^2 dq \\ &= \int_a^b \int_a^b \int_a^b c(r, q) c(s, q) f(s) f(r) ds dr dq = \int_a^b \int_a^b d(r, s) f(s) f(r) ds dr \\ &= \sum_{j=1}^K \lambda_j \langle \psi_j, f \rangle^2 \leq \lambda_l \sum_{j=l}^K \langle \psi_j, f \rangle^2 \leq \lambda_l, \end{aligned}$$

which implies the first statement. The second statement follows from the fact that $\int_a^b d(r, s) g(s) ds = 0$ because $g \in H_F^\perp$ and $\langle g, \psi_l \rangle = 0$ for all $l = 1, \dots, K$.

A.3 Auxiliary Lemmas

For the proofs of Theorems 1–3 we require some additional lemmas. Lemma A.1 is needed for Theorems 1–3, Lemma A.2 is needed for Theorems 2–3, Lemma A.3 is needed for

Theorem 2, Lemma A.4 is needed for Lemma A.5, and Lemma A.5 is needed for Theorem 3. The proofs of the lemmas can be found in Sections A.7–A.10.

Lemma A.1. *Under Assumptions 1–3, for any $0 \leq h < \infty$ and $i_1, i_2 = 0, \dots, h$, as $T \rightarrow \infty$, we have*

$$E \left[\left\| \frac{1}{T} \sum_{t=h+1}^T \tilde{F}_{t-i_1} \tilde{F}'_{t-i_2} - E \left[\tilde{F}_{t-i_1} \tilde{F}'_{t-i_2} \right] \right\|_M^2 \right] = O(T^{-1}).$$

Lemma A.2. *Under the conditions of Theorem 2, for any $0 \leq h < \infty$ and $i_1, i_2 = 0, \dots, h$, as $T \rightarrow \infty$,*

$$\left\| \frac{1}{T} \sum_{t=h+1}^T \hat{F}_{t-i_1}^{(K)} (\hat{F}_{t-i_2}^{(K)})' - \tilde{F}_{t-i_1} \tilde{F}'_{t-i_2} \right\|_M = O_P(T^{-1/2}).$$

Lemma A.3. *Under the conditions of Theorem 2, for any $0 \leq h < \infty$, $i, j = 0, \dots, h$, and $J \geq K$, as $T \rightarrow \infty$,*

$$\left\| \frac{1}{T} \sum_{t=h+1}^T \hat{F}_{t-i}^{(J)} (\hat{F}_{t-j}^{(J)})' - \hat{G}_{t,i,j} \right\|_M = O_P(T^{-1/2}),$$

where

$$\hat{G}_{t,i,j} := \begin{cases} \begin{bmatrix} \hat{F}_{t-i}^{(K)} (\hat{F}_{t-j}^{(K)})' & \mathbf{0}_{K,J-K} \\ \mathbf{0}_{J-K,K} & \mathbf{0}_{J-K,J-K} \end{bmatrix} & \text{for } i \neq j, \\ \begin{bmatrix} \hat{F}_{t-i}^{(K)} (\hat{F}_{t-i}^{(K)})' & \mathbf{0}_{K,J-K} \\ \mathbf{0}_{J-K,K} & \hat{V}_i \end{bmatrix} & \text{for } i = j, \end{cases}$$

and \hat{V}_i is defined as in Section A.1.

Lemma A.4. *Under the conditions of Theorem 2, for any $K \leq J \leq K_{\max}$ and $p \leq m \leq p_{\max}$, as $T \rightarrow \infty$,*

- (a) $\|T^{-1} \sum_{t=m+1}^T \hat{\mathbf{x}}_{t-1}^{(J,m)} \eta'_t\|_M = O_P(T^{-1/2})$
- (b) $\sum_{l=1}^J \|T^{-1} \sum_{t=m+1}^T \hat{\mathbf{x}}_{t-1}^{(J,m)} \langle \hat{\psi}_l, \epsilon_t^* \rangle\|_M = O_P(T^{-1/2})$
- (c) $\|T^{-1} \sum_{t=m+1}^T \hat{\mathbf{x}}_{t-1}^{(J,m)} (\tilde{\mathbf{x}}_{t-1} - \hat{\mathbf{x}}_{t-1}^{(K,p)})'\|_M = O_P(T^{-1/2})$

Lemma A.5. *Let $\Theta_P(\cdot)$ denote the exact order Landau symbol, that is, $a_T = \Theta_P(1)$ if and only if $a_T = O_P(1)$ and $a_T^{-1} = O_P(1)$. Under the conditions of Theorem 2, for any $J \leq K_{\max}$ and $m \leq p_{\max}$, as $T \rightarrow \infty$,*

$$\begin{aligned}
(a) \quad & \frac{1}{T} \sum_{t=m^*+1}^T \|\widehat{Y}_{t|t-1}^{(K,p)} - \widehat{Y}_{t|t-1}^{(J,m)}\|^2 = \begin{cases} O_P(T^{-1}) & \text{if } J \geq K \text{ and } m \geq p, \\ \Theta_P(1) & \text{otherwise,} \end{cases} \\
(b) \quad & \frac{1}{T} \sum_{t=m^*+1}^T \langle Y_t - \widetilde{Y}_{t|t-1}, \widehat{Y}_{t|t-1}^{(K,p)} - \widehat{Y}_{t|t-1}^{(J,m)} \rangle = \begin{cases} O_P(T^{-1}) & \text{if } J \geq K \text{ and } m \geq p, \\ O_P(T^{-1/2}) & \text{otherwise,} \end{cases} \\
(c) \quad & \frac{1}{T} \sum_{t=m^*+1}^T \langle \widetilde{Y}_{t|t-1} - \widehat{Y}_{t|t-1}^{(K,p)}, \widehat{Y}_{t|t-1}^{(K,p)} - \widehat{Y}_{t|t-1}^{(J,m)} \rangle = \begin{cases} O_P(T^{-1}) & \text{if } J \geq K \text{ and } m \geq p, \\ O_P(T^{-1/2}) & \text{otherwise.} \end{cases}
\end{aligned}$$

A.4 Proof of Theorem 1

Proof of Theorem 1(a)

Using sign-adjusted version of equation (A.1),

$$Y_t(r) = \mu(r) + (\widetilde{\Psi}(r))' \widetilde{F}_t + \epsilon_t^*(r), \quad (\text{A.5})$$

we have

$$\begin{aligned}
(\widehat{\mu}(r) - \mu(r))^2 &= \left((\widetilde{\Psi}(r))' \left(\frac{1}{T} \sum_{t=1}^T \widetilde{F}_t \right) + \frac{1}{T} \sum_{t=1}^T \epsilon_t^*(r) \right)^2 \\
&= \frac{1}{T^2} \left(\sum_{t=1}^T \widetilde{F}_t \right)' (\widetilde{\Psi}(r)) (\widetilde{\Psi}(r))' \left(\sum_{t=1}^T \widetilde{F}_t \right) + \frac{1}{T^2} \left(\sum_{t=1}^T \epsilon_t^*(r) \right)^2 \\
&\quad + \frac{2}{T^2} \left(\sum_{t=1}^T \widetilde{F}_t \right)' \left(\sum_{t=1}^T \widetilde{\Psi}(r) \epsilon_t^*(r) \right).
\end{aligned}$$

Since $\int_a^b \widetilde{\Psi}(r) \epsilon_t^*(r) dr = 0$ and $\int_a^b \widetilde{\Psi}(r) (\widetilde{\Psi}(r))' dr = \mathbf{0}_{K,K}$, it follows that

$$E[\|\widehat{\mu} - \mu\|^2] = \frac{1}{T^2} \sum_{t,h=1}^T E[\widetilde{F}_t' \widetilde{F}_h] + \frac{1}{T^2} \sum_{t,h=1}^T E[\langle \epsilon_t^*, \epsilon_h^* \rangle]. \quad (\text{A.6})$$

The first term of (A.6) satisfies

$$\frac{1}{T^2} \sum_{t,h=1}^T E[\widetilde{F}_t' \widetilde{F}_h] = \frac{1}{T^2} \sum_{t,h=1}^T \text{tr}(E[\widetilde{F}_t \widetilde{F}_h']) = \frac{1}{T^2} \sum_{t=1}^T \sum_{j=0}^{\infty} \text{tr}(B_i E[\eta_{t-i} \eta_{t-i}'] B_j') = O(T^{-1})$$

since

$$\frac{1}{T} \sum_{t=1}^T \sum_{i,j=0}^{\infty} \text{tr}(B_i E[\eta_{t-i} \eta_{t-i}'] B_j') \xrightarrow{T \rightarrow \infty} \sum_{i,j=0}^{\infty} \text{tr}(B_i \Sigma_{\eta} B_j') \leq \|\Sigma_{\eta}\|_M \sum_{i,j=0}^{\infty} \|B_i\|_M \|B_j\|_M < \infty$$

by Assumption 3(a) and the Cauchy-Schwarz inequality for the trace. For the second term of (A.6), note that ϵ_t^* is a m.d.s with respect to $\{\epsilon_{t-1}^*, \epsilon_{t-2}^*, \dots\}$ (see the discussion in Section A.1). Hence,

$$\frac{1}{T^2} \sum_{t,h=1}^T E[\langle \epsilon_t^*, \epsilon_h^* \rangle] = \frac{1}{T^2} \sum_{t=1}^T E[\|\epsilon_t^*\|^2] = O(T^{-1})$$

by Assumption 3(b). The assertion follows by Markov's inequality.

Proof of Theorem 1(b)

Consider the demeaned curves $Y_t^\mu(r) := Y_t(r) - \mu(r)$ and $\hat{Y}_t^\mu(r) := Y_t(r) - \hat{\mu}(r)$ yielding

$$c_\tau(r, s) = \lim_{T \rightarrow \infty} \frac{1}{T} \sum_{t=\tau+1}^T E[Y_t^\mu(r) Y_{t-\tau}^\mu(s)], \quad \hat{c}_\tau(r, s) = \frac{1}{T} \sum_{t=\tau+1}^T \hat{Y}_t^\mu(r) \hat{Y}_{t-\tau}^\mu(s).$$

Let \tilde{C}_τ be the integral operator with kernel

$$\tilde{c}_\tau(r, s) = \frac{1}{T} \sum_{t=\tau+1}^T Y_t^\mu(r) Y_{t-\tau}^\mu(s)$$

such that, by the triangle inequality,

$$\|\hat{C}_\tau - C_\tau\|_S \leq \|\hat{C}_\tau - \tilde{C}_\tau\|_S + \|\tilde{C}_\tau - C_\tau\|_S. \quad (\text{A.7})$$

It remains to show that the right-hand side of (A.7) is $O_P(T^{-1/2})$. For the first term of (A.7), we decompose

$$\begin{aligned} & \hat{Y}_t^\mu(r) \hat{Y}_{t-\tau}^\mu(s) - Y_t^\mu(r) Y_{t-\tau}^\mu(s) \\ &= \hat{Y}_t^\mu(r) (\hat{Y}_{t-\tau}^\mu(s) - Y_{t-\tau}^\mu(s)) + Y_{t-\tau}^\mu(s) (\hat{Y}_t^\mu(r) - Y_t^\mu(r)) \\ &= \hat{Y}_t^\mu(r) (\mu(s) - \hat{\mu}(s)) + Y_{t-\tau}^\mu(s) (\mu(r) - \hat{\mu}(r)) \\ &= (Y_t^\mu(r) + \mu(r) - \hat{\mu}(r)) (\mu(s) - \hat{\mu}(s)) + Y_{t-\tau}^\mu(s) (\mu(r) - \hat{\mu}(r)). \end{aligned}$$

Then,

$$\|\hat{C}_\tau - \tilde{C}_\tau\|_S^2 \leq \|A_1\|_S^2 + \|A_2\|_S^2 + 2\|A_1\|_S \|A_2\|_S,$$

where A_1, A_2 are the integral operators with kernels defined as:

$$\begin{aligned} a_1(r, s) &= \frac{1}{T} \sum_{t=\tau+1}^T (Y_t^\mu(r) + \mu(r) - \hat{\mu}(r))(\mu(s) - \hat{\mu}(s)), \\ a_2(r, s) &= \frac{1}{T} \sum_{t=\tau+1}^T Y_{t-\tau}^\mu(s)(\mu(r) - \hat{\mu}(r)). \end{aligned}$$

Hence, to derive the rate of convergence of $\|\hat{C}_\tau - \tilde{C}_\tau\|_S$ it suffices to obtain rates of convergence for $\|A_1\|_S$ and $\|A_2\|_S$. By Theorem 1(a), we have

$$\|A_1\|_S \leq \frac{1}{T} \sum_{t=\tau+1}^T \|(Y_t^\mu + \mu - \hat{\mu})\| \|\mu - \hat{\mu}\| = O_P(T^{-1/2})$$

because $T^{-1} \sum_{t=\tau+1}^T E\|(Y_t^\mu + \mu - \hat{\mu})\| \leq T^{-1} \sum_{t=\tau+1}^T E\|Y_t^\mu\| + E\|\mu - \hat{\mu}\| = O(1)$. By the identical arguments, it follows that $\|A_2\|_S = O_P(T^{-1/2})$, and $\|\hat{C}_\tau - \tilde{C}_\tau\|_S = O_P(T^{-1/2})$. For the second term of (A.7), we use the notation of equation (A.5) yielding

$$\begin{aligned} Y_t^\mu(r)Y_{t-\tau}^\mu(s) &= ((\tilde{\Psi}(r))' \tilde{F}_t + \epsilon_t^*(r))(\tilde{F}_{t-\tau}' \tilde{\Psi}(s) + \epsilon_{t-\tau}^*(s)), \\ E[Y_t^\mu(r)Y_{t-\tau}^\mu(s)] &= (\tilde{\Psi}(r))' E[\tilde{F}_t \tilde{F}_{t-\tau}'] \tilde{\Psi}(s) + (\tilde{\Psi}(r))' E[\tilde{F}_t \epsilon_{t-\tau}^*(s)], \end{aligned}$$

where the last equality follows from the m.d.s. property of ϵ_t^* . By the definition of the operators,

$$(\tilde{c}_\tau(r, s) - c_\tau(r, s))^2 = \lim_{T \rightarrow \infty} \left(\sum_{i=1}^4 b_i(r, s) \right)^2,$$

where

$$\begin{aligned} b_1(r, s) &= \frac{1}{T} \sum_{t=\tau+1}^T (\tilde{\Psi}(r))' (\tilde{F}_t \tilde{F}_{t-\tau}' - E[\tilde{F}_t \tilde{F}_{t-\tau}']) \tilde{\Psi}(s), \\ b_2(r, s) &= \frac{1}{T} \sum_{t=\tau+1}^T (\tilde{\Psi}(r))' (\tilde{F}_t \epsilon_{t-\tau}^*(s) - E[\tilde{F}_t \epsilon_{t-\tau}^*(s)]), \\ b_3(r, s) &= \frac{1}{T} \sum_{t=\tau+1}^T \epsilon_t^*(r) \tilde{F}_{t-\tau}' \tilde{\Psi}(s), \quad b_4(r, s) = \frac{1}{T} \sum_{t=\tau+1}^T \epsilon_t^*(r) \epsilon_{t-\tau}^*(s). \end{aligned}$$

Let B_i be the integral operator with kernel function $b_i(r, s)$. Then, by the triangle inequality,

$$\|\tilde{C}_\tau - C_\tau\|_S^2 = \int_a^b \int_a^b (\tilde{c}_\tau(r, s) - c_\tau(r, s))^2 ds dr \leq \lim_{T \rightarrow \infty} \sum_{i,j=1}^4 \|B_i\|_S \|B_j\|_S.$$

Hence, it remains to show that $\|B_i\|_S = O_P(T^{-1/2})$ for $i = 1, \dots, 4$. For the first operator, define

$$G_1 := \frac{1}{T} \sum_{t=\tau+1}^T (\tilde{F}_t \tilde{F}'_{t-\tau} - E[\tilde{F}_t \tilde{F}'_{t-\tau}]).$$

By the Cauchy-Schwarz inequality,

$$(b_1(r, s))^2 = ((\tilde{\Psi}(r))' G_1 \tilde{\Psi}(s))^2 = (\tilde{\Psi}(r))' G_1 \tilde{\Psi}(s) (\tilde{\Psi}(s))' G_1' \tilde{\Psi}(r),$$

and, since the loading functions are orthonormal,

$$\begin{aligned} \|B_1\|_S^2 &= \int_a^b (\tilde{\Psi}(r))' G_1 G_1' \tilde{\Psi}(r) dr = \int_a^b \text{tr} \left(G_1 G_1' \tilde{\Psi}(r) (\tilde{\Psi}(r))' \right) dr \\ &= \text{tr} (G_1 G_1') = \|G_1\|_M^2 = O_P(T^{-1/2}), \end{aligned}$$

where the last step follows from Lemma A.1. For the second operator,

$$\|B_2\|_S = \sqrt{\int_a^b \left\| \frac{1}{T} \sum_{t=\tau+1}^T \tilde{F}_t \epsilon_{t-\tau}^*(s) \right\|_2^2 ds} = O_P(T^{-1/2})$$

since $E[\|B_2\|_S] = O(T^{-1/2})$ by Assumption 3(b) and Jensen's inequality. For the third operator,

$$\|B_3\|_S^2 = \int_a^b \sum_{l=1}^K \left(\frac{1}{T} \sum_{t=\tau+1}^T \tilde{F}_{l,t-\tau} \epsilon_t^*(s) \right)^2 ds$$

and $E[(T^{-1} \sum_{t=\tau+1}^T \tilde{F}_{l,t-\tau} \epsilon_t^*(s))^2] = T^{-2} \sum_{t=\tau+1}^T E[\tilde{F}_{l,t}^2 (\epsilon_t^*(s))^2] = O(T^{-1})$ by Assumption 1(a) and the fact that the fourth moments are bounded. Hence, $\|B_3\|_S = O_P(T^{-1/2})$. Finally, for the fourth operator,

$$\begin{aligned} E\|B_4\|_S^2 &\leq \int_a^b \int_a^b E \left[\left(\frac{1}{T} \sum_{t=\tau+1}^T \epsilon_t^*(r) \epsilon_{t-\tau}^*(s) \right)^2 \right] ds dr \\ &= \frac{1}{T^2} \sum_{t=\tau+1}^T E[\|\epsilon_t^*\| \|\epsilon_{t-\tau}^*\|] + \frac{2}{T} \sum_{t=\tau+2}^T \sum_{h=\tau+1}^{t-1} E[\langle \epsilon_t^*, \epsilon_{t-h}^* \rangle \langle \epsilon_{t-\tau}^*, \epsilon_{t-\tau-h}^* \rangle], \quad (\text{A.8}) \end{aligned}$$

where the first term of (A.8) is $O_P(T^{-1})$ by Assumption 3(b). As discussed in the proof of Theorem 1(a), from Assumption 1(a) it follows that ϵ_t^* is m.d.s with respect to $\{\epsilon_{t-1}^*, \epsilon_{t-2}^*, \dots\}$. Hence, for the second term, $E[\langle \epsilon_t^*, \epsilon_{t-h}^* \rangle \langle \epsilon_{t-\tau}^*, \epsilon_{t-\tau-h}^* \rangle] = 0$ for $\tau > 0$ and $h = \tau + 1, \dots, t - 1$ by m.d.s property and the law of iterated expectation. Consequently, $\|B_4\|_{\mathcal{S}} = O_P(T^{-1/2})$, and the right-hand side of (A.7) is $O_P(T^{-1/2})$ by Markov's inequality.

Proof of Theorem 1(c)

We have the decomposition

$$\begin{aligned} & \widehat{c}_\tau(r, q) \widehat{c}_\tau(s, q) - c_\tau(r, q) c_\tau(s, q) \\ &= (\widehat{c}_\tau(r, q) - c_\tau(r, q)) \widehat{c}_\tau(s, q) + (\widehat{c}_\tau(s, q) - c_\tau(s, q)) c_\tau(r, q) \\ &= (\widehat{c}_\tau(r, q) - c_\tau(r, q)) (\widehat{c}_\tau(s, q) - c_\tau(s, q)) \\ &\quad + (\widehat{c}_\tau(r, q) - c_\tau(r, q)) c_\tau(s, q) + (\widehat{c}_\tau(s, q) - c_\tau(s, q)) c_\tau(r, q), \end{aligned}$$

which implies that $\widehat{D} - D = \sum_{\tau=1}^{q_0} (A_{\tau,1} + A_{\tau,2} + A_{\tau,3})$, where $A_{\tau,1}$ is the integral operator with kernel function

$$a_{\tau,1}(r, s) = \int_a^b (\widehat{c}_\tau(r, q) - c_\tau(r, q)) (\widehat{c}_\tau(s, q) - c_\tau(s, q)) dq,$$

$A_{\tau,2}$ is the integral operator with kernel function

$$a_{\tau,2}(r, s) = \int_a^b (\widehat{c}_\tau(r, q) - c_\tau(r, q)) c_\tau(s, q) dq,$$

and $A_{\tau,3}$ is the integral operator with kernel function $a_{\tau,3}(r, s) = a_{\tau,2}(s, r)$. The Cauchy-Schwarz inequality implies

$$\begin{aligned} (a_{\tau,1}(r, s))^2 &\leq \left(\int_a^b (\widehat{c}_\tau(r, q) - c_\tau(r, q))^2 dq \right) \left(\int_a^b (\widehat{c}_\tau(s, q) - c_\tau(s, q))^2 dq \right) \\ (a_{\tau,2}(r, s))^2 &\leq \left(\int_a^b (\widehat{c}_\tau(r, q) - c_\tau(r, q))^2 dq \right) \left(\int_a^b (c_\tau(s, q))^2 dq \right). \end{aligned}$$

Assumption 1(b) implies that $\int_a^b (c_\tau(r, q))^2 dq = (\Psi(r))' M(\Psi(r))$, which is continuous in r by Assumption 1(c). Therefore, $\sup_{r \in [a, b]} \int_a^b (c_\tau(r, q))^2 dq < \infty$, and it follows that

$$\|A_{\tau,1}\|_{\mathcal{S}} + \|A_{\tau,2}\|_{\mathcal{S}} + \|A_{\tau,3}\|_{\mathcal{S}} = O_P(\|\widehat{C}_\tau - C_\tau\|_{\mathcal{S}}),$$

and

$$\|\widehat{D} - D\|_{\mathcal{S}} \leq \sum_{\tau=1}^{q_0} (\|A_{\tau,1}\|_{\mathcal{S}} + \|A_{\tau,2}\|_{\mathcal{S}} + \|A_{\tau,3}\|_{\mathcal{S}}) = O_P(T^{-1/2}).$$

Proof of Theorem 1(d)

Lemma 2.2 in Horváth and Kokoszka (2012) implies $|\widehat{\lambda}_l - \lambda_l| \leq \|\widehat{D} - D\|_{\mathcal{S}}$ for all $l = 1, \dots, K$ and $|\widehat{\lambda}_l| \leq \|\widehat{D} - D\|_{\mathcal{S}}$ for all $l > K$. Then, the result follows from (c).

Proof of Theorem 1(e)

Lemma 2.3 in Horváth and Kokoszka (2012) implies

$$\max_{1 \leq l \leq K} \|s_l \widehat{\psi}_l - \psi_l\| \leq \frac{2\sqrt{2}}{\alpha} \|\widehat{D} - D\|_{\mathcal{S}},$$

where $\alpha = \min\{\lambda_1 - \lambda_2, \lambda_2 - \lambda_3, \dots, \lambda_{K-1} - \lambda_K, \lambda_K\}$, and the result follows from (c).

A.5 Proof of Theorem 2

Proof of Theorem 2(a)

With the notations introduced in Section A.1, we have

$$\|\widehat{\Gamma}_{(J,m)} - \widetilde{\Gamma}^*\|_M^2 = \sum_{i=1}^m \left\| \frac{1}{T} \sum_{t=m+1}^T \widehat{F}_t^{(J)} (\widehat{F}_{t-i}^{(J)})' - \mathbf{R}'_{K,J} E[\widetilde{F}_t \widetilde{F}_{t-i}'] \mathbf{R}_{K,J} \right\|_M^2,$$

and the triangle inequality implies

$$\left\| \frac{1}{T} \sum_{t=m+1}^T \widehat{F}_t^{(J)} (\widehat{F}_{t-i}^{(J)})' - \mathbf{R}'_{K,J} E[\widetilde{F}_t \widetilde{F}_{t-i}'] \mathbf{R}_{K,J} \right\|_M \leq M_1 + M_2 + M_3$$

with

$$\begin{aligned} M_1 &= \left\| \frac{1}{T} \sum_{t=m+1}^T \widehat{F}_t^{(J)} (\widehat{F}_{t-i}^{(J)})' - \mathbf{R}'_{K,J} \widehat{F}_t^{(K)} (\widehat{F}_{t-i}^{(K)})' \mathbf{R}_{K,J} \right\|_M, \\ M_2 &= \left\| \frac{1}{T} \sum_{t=m+1}^T \mathbf{R}'_{K,J} \widehat{F}_t^{(K)} (\widehat{F}_{t-i}^{(K)})' \mathbf{R}_{K,J} - \mathbf{R}'_{K,J} \widetilde{F}_t \widetilde{F}_{t-i}' \mathbf{R}_{K,J} \right\|_M, \\ M_3 &= \left\| \frac{1}{T} \sum_{t=m+1}^T \mathbf{R}'_{K,J} \widetilde{F}_t \widetilde{F}_{t-i}' \mathbf{R}_{K,J} - \mathbf{R}'_{K,J} E[\widetilde{F}_t \widetilde{F}_{t-i}'] \mathbf{R}_{K,J} \right\|_M. \end{aligned}$$

Using the notation introduced in Lemma A.3, we have $\mathbf{R}'_{K,J} \widehat{F}_t^{(K)} (\widehat{F}_{t-i}^{(K)})' \mathbf{R}_{K,J} = \widehat{G}_{t,0,i}$ with $i \geq 1$. Then, Lemma A.3 implies $M_1 = O_P(T^{-1/2})$. Due to the block structure of zeros

generated by $\mathbf{R}_{K,J}$, we have $M_2 = \|T^{-1} \sum_{t=m+1}^T \hat{F}_t^{(K)} (\hat{F}_{t-i}^{(K)})' - \tilde{F}_t (\tilde{F}_{t-i})'\|_M = O_P(T^{-1/2})$ by Lemma A.2, and $M_3 = \|T^{-1} \sum_{t=m+1}^T \tilde{F}_t (\tilde{F}_{t-i})' - E[\tilde{F}_t (\tilde{F}_{t-i})']\|_M = O_P(T^{-1/2})$ by Lemma A.1, which implies

$$\|\hat{\Gamma}_{(J,m)} - \tilde{\Gamma}^*\|_M = O_P(T^{-1/2}).$$

Analogously,

$$\|\hat{\Sigma}_{(J,m)} - \tilde{\Sigma}^*\|_M^2 = \sum_{i_1, i_2=1}^m \left\| \frac{1}{T} \sum_{t=m+1}^T \hat{F}_{t-i_1}^{(J)} (\hat{F}_{t-i_2}^{(J)})' - G_{i_1, i_2} \right\|_M^2,$$

where

$$\left\| \frac{1}{T} \sum_{t=m+1}^T \hat{F}_{t-i_1}^{(J)} (\hat{F}_{t-i_2}^{(J)})' - G_{i_1, i_2} \right\|_M \leq M_4 + M_5 + M_6,$$

and, by Lemmas A.1–A.3, the terms on the right hand side satisfy

$$\begin{aligned} M_4 &= \left\| \frac{1}{T} \sum_{t=m+1}^T \hat{F}_{t-i_1}^{(J)} (\hat{F}_{t-i_2}^{(J)})' - \hat{G}_{t, i_1, i_2} \right\|_M = O_P(T^{-1/2}), \\ M_5 &= \left\| \frac{1}{T} \sum_{t=m+1}^T \hat{F}_{t-i_1}^{(K)} (\hat{F}_{t-i_2}^{(K)})' - \tilde{F}_{t-i_1} \tilde{F}_{t-i_2}' \right\|_M = O_P(T^{-1/2}), \\ M_6 &= \left\| \frac{1}{T} \sum_{t=m+1}^T \tilde{F}_{t-i_1} \tilde{F}_{t-i_2}' - E[\tilde{F}_{t-i_1} \tilde{F}_{t-i_2}'] \right\|_M = O_P(T^{-1/2}). \end{aligned}$$

Consequently, $\|\hat{\Sigma}_{(J,m)} - \tilde{\Sigma}^*\|_M = O_P(T^{-1/2})$. Note that $\|\hat{\Gamma}_{(J,m)}\|_M = O_P(1)$, and, since $\tilde{\Sigma}^*$ is uniformly positive definite, $\|(\tilde{\Sigma}^*)^{-1}\|_M = O_P(1)$. Following the proof of Lemma 3 in Berk (1974) we define $q = \hat{\Sigma}_{(J,m)}^{-1} - (\tilde{\Sigma}^*)^{-1}$. Then,

$$q = (\tilde{\Sigma}_{(J,m)}^{-1} + q)((\tilde{\Sigma}^*)^{-1} - \hat{\Sigma}_{(J,m)})(\tilde{\Sigma}^*)^{-1},$$

which implies that

$$\|q\|_M^2 \leq \frac{\|(\tilde{\Sigma}^*)^{-1}\|_M^2 \|(\tilde{\Sigma}^*)^{-1} - \hat{\Sigma}_{(J,m)}\|_M}{1 - \|(\tilde{\Sigma}^*)^{-1}\|_M \|(\tilde{\Sigma}^*)^{-1} - \hat{\Sigma}_{(J,m)}\|_M}. \quad (\text{A.9})$$

The numerator of (A.9) is $O_P(T^{-1/2})$, and the denominator is bounded away from zero, which implies that

$$\|\hat{\Sigma}_{(J,m)}^{-1} - (\tilde{\Sigma}^*)^{-1}\|_M = O_P(T^{-1/2}).$$

Consider the decomposition

$$\hat{\mathbf{A}}^* - \mathbf{A}^* = \hat{\Gamma}_{(J,m)} (\hat{\Sigma}_{(J,m)}^{-1} - (\tilde{\Sigma}^*)^{-1}) + (\hat{\Gamma}_{(J,m)} - \tilde{\Gamma}^*) (\tilde{\Sigma}^*)^{-1}.$$

Then, by the triangle inequality and by putting together all rates, we obtain

$$\begin{aligned}\|\hat{\mathbf{A}}^* - \mathbf{A}^*\|_M &\leq \|\hat{\Gamma}_{(J,m)}\|_M \|\hat{\Sigma}_{(J,m)}^{-1} - (\tilde{\Sigma}^*)^{-1}\|_M + \|\hat{\Gamma}_{(J,m)} - \tilde{\Gamma}^*\|_M \|(\tilde{\Sigma}^*)^{-1}\|_M \\ &= O_P(T^{-1/2}).\end{aligned}$$

Proof of Theorem 2(b)

In the first scenario, $m < p$, we have

$$\begin{aligned}\mathbf{A}^* &= [\mathbf{R}'_{K,J} \tilde{A}_1 \mathbf{R}_{K,J}, \dots, \mathbf{R}'_{K,J} \tilde{A}_p \mathbf{R}_{K,J}], \\ \hat{\mathbf{A}}^* &= [\mathbf{R}'_{J,K} \hat{A}_1^{(J)} \mathbf{R}_{J,K}, \dots, \mathbf{R}'_{J,K} \hat{A}_m^{(J)} \mathbf{R}_{J,K}, \mathbf{0}_{J^*, (p-m)J^*}].\end{aligned}$$

Then, for any T ,

$$\begin{aligned}\|\hat{\mathbf{A}}^* - \mathbf{A}^*\|_M^2 &= \sum_{i=1}^m \|\mathbf{R}'_{J,K} \hat{A}_i^{(J)} \mathbf{R}_{J,K} - \mathbf{R}'_{K,J} \tilde{A}_i \mathbf{R}_{K,J}\|_M^2 + \sum_{i=m+1}^p \|\mathbf{R}'_{K,J} \tilde{A}_i \mathbf{R}_{K,J}\|_M^2 \\ &\geq \sum_{i=m+1}^p \|\mathbf{R}'_{K,J} \tilde{A}_i \mathbf{R}_{K,J}\|_M^2 = \sum_{i=m+1}^p \|A_i\|_M^2 > 0,\end{aligned}$$

where the last inequality follows from the fact that $A_p \neq 0$ by Assumption 3(a).

In the scenario $J < K$ and $m \geq p$ we have

$$\mathbf{A}^* = [\tilde{A}_1, \dots, \tilde{A}_p, \mathbf{0}_{J, (m-p)J}], \quad \hat{\mathbf{A}}^* = [\mathbf{R}'_{J,K} \hat{A}_1^{(J)} \mathbf{R}_{J,K}, \dots, \mathbf{R}'_{J,K} \hat{A}_m^{(J)} \mathbf{R}_{J,K}].$$

The first Kp elements of the last row of \mathbf{A}^* coincide with those of $\tilde{\mathbf{A}}$ and are given by $\mathbf{a} = E[\tilde{\mathbf{x}}_{t-1} \tilde{\mathbf{x}}'_{t-1}]^{-1} E[\tilde{\mathbf{x}}_{t-1} \tilde{F}_{K,t}]$, which are the population coefficients of the regression of $\tilde{F}_{K,t}$ on $\tilde{F}_{t-1}, \dots, \tilde{F}_{t-p}$. Assumption 1(b) implies that $\|\mathbf{a}\|_2 > 0$. The first Kp elements of the last row of $\hat{\mathbf{A}}^*$ are zero since $J < K$. Therefore,

$$\|\hat{\mathbf{A}}^* - \mathbf{A}^*\|_M^2 \geq \|\mathbf{a}\|_2^2 > 0.$$

A.6 Proof of Theorem 3

Note that \hat{K} and \hat{p} are discrete random variables. Therefore, to prove Theorem 3, it is sufficient to show that

$$\lim_{T \rightarrow \infty} \mathbb{P}(\text{CR}_T(J, m) < \text{CR}_T(K, p)) = 0$$

for all $J \leq K_{max}$ and $m \leq p_{max}$. From the definition of the information criterion, we have

$$CR_T(J, m) - CR_T(K, p) = MSE_T(J, m) - MSE_T(K, p) + g_T(J, m) - g_T(K, p).$$

Without loss of generality, we prove the result for the case when $f(x) = x$ as the proof for any other strictly increasing transformation $f(\cdot)$ is identical. Hence, it remains to show that

$$\lim_{T \rightarrow \infty} P\left(MSE_T(K, p) - MSE_T(J, m) > g_T(J, m) - g_T(K, p)\right) = 0.$$

We split the proof into case I, the case of overselection ($J \geq K$ and $m \geq p$), and case II, the case of underselection ($J < K$ or $m < p$ or both). In any of the two cases, we have

$$MSE_T(J, m) = \frac{1}{T - m} \sum_{t=m+1}^T \|Y_t - \hat{Y}_{t|t-1}^{(J,m)}\|^2 = O_P(1),$$

which follows from representations (A.2) and (A.3) together with Theorem 1(a), Theorem 2, Lemma A.2, and the fact that enough moments are bounded. Moreover, we have $MSE_T(J, m) - T^{-1}(T - m)MSE_T(J, m) = O_P(T^{-1})$, and

$$\begin{aligned} & \frac{T - m}{T} MSE_T(J, m) - \frac{T - p}{T} MSE_T(K, p) - \frac{1}{T} \sum_{t=m^*+1}^T \left(\|Y_t - \hat{Y}_{t|t-1}^{(J,m)}\|^2 - \|Y_t - \hat{Y}_{t|t-1}^{(K,p)}\|^2 \right) \\ &= \frac{1}{T} \sum_{t=m+1}^{m^*} \|Y_t - \hat{Y}_{t|t-1}^{(J,m)}\|^2 - \frac{1}{T} \sum_{t=p+1}^{m^*} \|Y_t - \hat{Y}_{t|t-1}^{(K,p)}\|^2 = O_P(T^{-1}), \end{aligned}$$

where $m^* = \max\{m, p\}$, which implies that, for any of the two cases I and II,

$$MSE_T(J, m) - MSE_T(K, p) = \frac{1}{T} \sum_{t=m^*+1}^T \left(\|Y_t - \hat{Y}_{t|t-1}^{(J,m)}\|^2 - \|Y_t - \hat{Y}_{t|t-1}^{(K,p)}\|^2 \right) + O_P(T^{-1}).$$

Hence, it remains to study $T^{-1} \sum_{t=m^*+1}^T (\|Y_t - \hat{Y}_{t|t-1}^{(J,m)}\|^2 - \|Y_t - \hat{Y}_{t|t-1}^{(K,p)}\|^2)$. A useful decomposition is obtained by adding and subtracting $\hat{Y}_{t|t-1}^{(K,p)}$, i.e.,

$$\begin{aligned} & \|Y_t - \hat{Y}_{t|t-1}^{(J,m)}\|^2 - \|Y_t - \hat{Y}_{t|t-1}^{(K,p)}\|^2 \\ &= \|Y_t - \hat{Y}_{t|t-1}^{(K,p)} + \hat{Y}_{t|t-1}^{(K,p)} - \hat{Y}_{t|t-1}^{(J,m)}\|^2 - \|Y_t - \hat{Y}_{t|t-1}^{(K,p)}\|^2 \\ &= \|\hat{Y}_{t|t-1}^{(K,p)} - \hat{Y}_{t|t-1}^{(J,m)}\|^2 + 2\langle Y_t - \hat{Y}_{t|t-1}^{(K,p)}, \hat{Y}_{t|t-1}^{(K,p)} - \hat{Y}_{t|t-1}^{(J,m)} \rangle, \end{aligned}$$

and Lemma A.5 implies

$$\frac{1}{T} \sum_{t=m^*+1}^T \left(\|Y_t - \hat{Y}_{t|t-1}^{(J,m)}\|^2 - \|\hat{Y}_{t|t-1}^{(K,p)} - \hat{Y}_{t|t-1}^{(J,m)}\|^2 \right) = \begin{cases} O_P(T^{-1}) & \text{for case I,} \\ \Theta_P(1) & \text{for case II,} \end{cases}$$

so that

$$MSE_T(J, m) - MSE_T(K, p) = \begin{cases} O_P(T^{-1}) & \text{for case I,} \\ \Theta_P(1) & \text{for case II.} \end{cases} \quad (\text{A.10})$$

For case I, if $J \geq K$ and $m > p$ or $J > K$ and $m \geq p$, we have $g_T(J, m) - g_T(K, p) > 0$, which converges to zero at a slower rate than T^{-1} . This follows from the condition that $Tg_T(J, m) \rightarrow \infty$ as $T \rightarrow \infty$ for all J and m . Thus, $P(\text{CR}_T(J, m) < \text{CR}_T(K, p)) \rightarrow 0$ as $T \rightarrow \infty$. This result is trivially satisfied if $(J, m) = (K, p)$. For case II, (A.10) implies $\text{plim}_{T \rightarrow \infty}(MSE_T(K, p) - MSE_T(J, m)) > 0$, which yields

$$\text{plim}_{T \rightarrow \infty} (MSE_T(K, p) - MSE_T(L, m)) < 0.$$

Since $\lim_{T \rightarrow \infty}(g_T(L, m) - g_T(K, p)) = 0$, which is implied by the condition that $g_T(J, m) \rightarrow 0$ for all J and m , it follows that $P(\text{CR}_T(J, m) < \text{CR}_T(K, p)) \rightarrow 0$ as $T \rightarrow \infty$, which concludes the proof of the theorem.

A.7 Proof of Lemma A.1

The expression of interest can be rewritten as

$$\begin{aligned} & E \left[\left\| \frac{1}{T} \sum_{t=h+1}^T \tilde{F}_{t-i_1} \tilde{F}'_{t-i_2} - E[\tilde{F}_{t-i_1} \tilde{F}'_{t-i_2}] \right\|_M^2 \right] \\ &= \frac{1}{T^2} \sum_{t,s=h+1}^T \sum_{m,l=1}^K \text{Cov}[\tilde{F}_{m,t-i_1} \tilde{F}_{l,t-i_2}, \tilde{F}_{m,s-i_1} \tilde{F}_{l,s-i_2}]. \end{aligned} \quad (\text{A.11})$$

Since the $\text{VAR}(p)$ process \tilde{F}_t is causal by Assumption 3(a), it has the vector moving average representation $\tilde{F}_t = \sum_{j=0}^{\infty} B_j \eta_{t-j}$, where $\sum_{j=0}^{\infty} \|B_j\|_M < \infty$, or, equivalently

$$\tilde{F}_{l,t} = \sum_{j=0}^{\infty} \sum_{k=1}^K b_j^{(l,k)} \eta_{k,t-j},$$

where $b_j^{(l,k)}$ is the (l, k) element of the matrix B_j and $\eta_{k,t-j}$ is the k -th element of the vector η_{t-j} . Then, $Cov[\tilde{F}_{m,t-i_1}\tilde{F}_{l,t-i_2}, \tilde{F}_{m,s-i_1}\tilde{F}_{l,s-i_2}]$ is equal to

$$\sum_{j_1, j_2, j_3, j_4=0}^{\infty} \sum_{k_1, k_2, k_3, k_4=1}^K b_{j_1}^{(m, k_1)} b_{j_2}^{(l, k_2)} b_{j_3}^{(m, k_3)} b_{j_4}^{(l, k_4)} Cov[\eta_{k_1, t-i_1-j_1} \eta_{k_2, t-i_2-j_2}, \eta_{k_3, s-i_1-j_3} \eta_{k_4, s-i_2-j_4}].$$

By Assumption 3(a), there exists a constant $\kappa < \infty$ such that

$$\lim_{T \rightarrow \infty} \sup_{j_1, j_2, j_3, j_4 \in \mathbb{N}} \frac{1}{T} \left| \sum_{t, s=h+1}^T Cov[\eta_{k_1, t-i_1-j_1} \eta_{k_2, t-i_2-j_2}, \eta_{k_3, s-i_1-j_3} \eta_{k_4, s-i_2-j_4}] \right| \leq \kappa.$$

Equation (A.11) and the triangle inequality imply

$$\lim_{T \rightarrow \infty} E \left[\left\| \frac{1}{\sqrt{T}} \sum_{t=h+1}^T \tilde{F}_{t-i_1} \tilde{F}'_{t-i_2} - E[\tilde{F}_{t-i_1} \tilde{F}'_{t-i_2}] \right\|_M^2 \right] \leq K^6 \kappa \left(\sum_{j=0}^{\infty} \|B_j\|_{\infty} \right)^4 < \infty,$$

where $\|A\|_{\infty} = \max_{i,j} \{|a_{i,j}|\}$ is the maximum norm satisfying the matrix inequality $\|A\|_{\infty} \leq \|A\|_M$ (see, e.g., Lütkepohl 1996 Section 8.5.2). Consequently, (A.11) is $O(T^{-1})$.

A.8 Proof of Lemma A.2

We split our proof in two parts. In the first part we focus on the estimation error for the mean function and show that

$$\left\| \frac{1}{T} \sum_{t=h+1}^T \hat{F}_{t-i_1}^{(K)} (\hat{F}_{t-i_2}^{(K)})' - \check{F}_{t-i_1} \check{F}'_{t-i_2} \right\|_M = O_P(T^{-1/2}), \quad (\text{A.12})$$

where $\check{F}_t = (\check{F}_{1,t}, \dots, \check{F}_{K,t})'$ with $\check{F}_{l,t} = \langle Y_t - \mu, \hat{\psi}_l \rangle$, and in the second part, we show that

$$\left\| \frac{1}{T} \sum_{t=h+1}^T \check{F}_{t-i_1} \check{F}'_{t-i_2} - \tilde{F}_{t-i_1} \tilde{F}'_{t-i_2} \right\|_M = O_P(T^{-1/2}). \quad (\text{A.13})$$

The final result then follows by the triangle inequality. To show equation (A.12), we define $\check{R}_t = \hat{F}_t^{(K)} - \check{F}_t$ and decompose the expression of interest as

$$\begin{aligned} \|\hat{F}_{t-i_1}^{(K)} (\hat{F}_{t-i_2}^{(K)})' - \check{F}_{t-i_1} \check{F}'_{t-i_2}\|_M^2 &= \|\check{R}_{t-i_1} (\hat{F}_{t-i_2}^{(K)})' + \check{F}_{t-i_1} \check{R}'_{t-i_2}\|_M^2 \\ &= \|\check{R}_{t-i_1} \check{R}'_{t-i_2} + \check{R}_{t-i_1} \check{F}'_{t-i_2} + \check{F}_{t-i_1} \check{R}'_{t-i_2}\|_M^2 \\ &= \|\check{R}_{t-i_1}\|_2^2 \|\check{R}_{t-i_2}\|_2^2 + \|\check{R}_{t-i_1}\|_2^2 \|\check{F}_{t-i_2}\|_2^2 + \|\check{F}_{t-i_1}\|_2^2 \|\check{R}_{t-i_2}\|_2^2, \end{aligned}$$

where the last step follows by the definitions of the Frobenius and the Euclidean norm. The Cauchy-Schwarz inequality and the fact that the estimated loadings have unit norm imply

$$\|\check{R}_t\|_2^2 = \sum_{l=1}^K |\hat{F}_{l,t} - \check{F}_{l,t}|^2 = \sum_{l=1}^K |\langle \mu - \hat{\mu}, \hat{\psi}_l \rangle|^2 \leq K \|\mu - \hat{\mu}\|^2$$

for any t . Consequently, by the triangle inequality,

$$\begin{aligned} & \left\| \frac{1}{T} \sum_{t=h+1}^T \hat{F}_{t-i_1}^{(K)} (\hat{F}_{t-i_2}^{(K)})' - \check{F}_{t-i_1} \check{F}_{t-i_2}' \right\|_M \\ & \leq \frac{1}{T} \sum_{t=h+1}^T \left\| \hat{F}_{t-i_1}^{(K)} (\hat{F}_{t-i_2}^{(K)})' - \check{F}_{t-i_1} \check{F}_{t-i_2}' \right\|_M \\ & \leq \|\mu - \hat{\mu}\| \frac{\sqrt{K}}{T} \sum_{t=h+1}^T \sqrt{K \|\mu - \hat{\mu}\|^2 + \|\check{F}_{t-i_1}\|_2^2 + \|\check{F}_{t-i_2}\|_2^2}, \end{aligned}$$

and (A.12) follows by Theorem 1(a) and the fact that enough moments of the factors are bounded. Analogously, to show (A.13), we define $R_t := \check{F}_t - \tilde{F}_t$ and decompose

$$\check{F}_{t-i_1} \check{F}_{t-i_2}' - \tilde{F}_{t-i_1} \tilde{F}_{t-i_2}' = R_{t-i_1} R_{t-i_2}' + R_{t-i_1} \tilde{F}_{t-i_2}' + \tilde{F}_{t-i_1} R_{t-i_2}'.$$

By the triangle inequality, it remains to show that

$$\left\| \frac{1}{T} \sum_{t=h+1}^T R_{t-i_1} R_{t-i_2}' \right\|_M = O_P(T^{-1/2}), \quad \left\| \frac{1}{T} \sum_{t=h+1}^T \tilde{F}_{t-i_1} R_{t-i_2}' \right\|_M = O_P(T^{-1/2}). \quad (\text{A.14})$$

Note that the l -th entry of R_t is $R_{l,t} = \langle Y_t - \mu, \hat{\psi}_l - \tilde{\psi}_l \rangle$. Then, the Cauchy-Schwarz inequality implies

$$\begin{aligned} & \left\| \frac{1}{T} \sum_{t=h+1}^T R_{t-i_1} R_{t-i_2}' \right\|_M^2 = \sum_{k,l=1}^K \left(\frac{1}{T} \sum_{t=h+1}^T \langle Y_{t-i_1} - \mu, \hat{\psi}_k - \tilde{\psi}_k \rangle \langle Y_{t-i_2} - \mu, \hat{\psi}_l - \tilde{\psi}_l \rangle \right)^2 \\ & \leq \sum_{k,l=1}^K \left(\frac{1}{T} \sum_{t=h+1}^T \langle Y_{t-i_1} - \mu, \hat{\psi}_k - \tilde{\psi}_k \rangle^2 \right) \left(\frac{1}{T} \sum_{t=h+1}^T \langle Y_{t-i_2} - \mu, \hat{\psi}_l - \tilde{\psi}_l \rangle^2 \right) \\ & \leq \left(\sum_{k,l=1}^K \|\hat{\psi}_k - \tilde{\psi}_k\|^2 \|\hat{\psi}_l - \tilde{\psi}_l\|^2 \right) \left(\frac{1}{T} \sum_{t=h+1}^T \|Y_{t-i_1} - \mu\|^2 \right) \left(\frac{1}{T} \sum_{t=h+1}^T \|Y_{t-i_2} - \mu\|^2 \right). \end{aligned}$$

Theorem 1(e), Slutsky's theorem, and the fact that $T^{-1} \sum_{t=h+1}^T \|Y_{t-i_1} - \mu\|^2 = O_P(1)$ since enough moments are bounded imply that the term above is $O_P(T^{-2})$, which implies

the first statement in (A.14). Similarly,

$$\begin{aligned} \left\| \frac{1}{T} \sum_{t=h+1}^T \tilde{F}_{t-i_1} R'_{t-i_2} \right\|_M^2 &= \sum_{k,l=1}^K \left\langle \frac{1}{T} \sum_{t=h+1}^T \tilde{F}_{k,t-i_1} (Y_{t-i_2} - \mu), \hat{\psi}_l - \tilde{\psi}_l \right\rangle^2 \\ &\leq \left(\sum_{l=1}^K \|\hat{\psi}_l - \tilde{\psi}_l\|^2 \right) \left(\sum_{k=1}^K \left\| \frac{1}{T} \sum_{t=h+1}^T \tilde{F}_{k,t-i_1} (Y_{t-i_2} - \mu) \right\|^2 \right) = O_P(T^{-1}), \end{aligned}$$

where the last step follows from Theorem 1(e) and the fact that enough moments are bounded. Consequently, (A.14) and (A.13) hold, and the assertion follows.

A.9 Proof of Lemma A.3

The expression $T^{-1} \sum_{t=h+1}^T \hat{F}_{t-i}^{(J)} (\hat{F}_{t-j}^{(J)})' - \hat{G}_{t,i,j}$ can be partitioned into four blocks: the top left block is $\mathbf{0}_{K,K}$, the top right block is $T^{-1} \sum_{t=h+1}^T \hat{F}_{t-i}^{(K)} (\hat{F}_{K+1,t-j}, \dots, \hat{F}_{J,t-j})$, the bottom left block is $T^{-1} \sum_{t=h+1}^T (\hat{F}_{K+1,t-i}, \dots, \hat{F}_{J,t-i})' \hat{F}_{t-j}^{(K)}$, and, for the case $i \neq j$, the bottom right block is $T^{-1} \sum_{t=h+1}^T (\hat{F}_{K+1,t-i}, \dots, \hat{F}_{J,t-i})' (\hat{F}_{K+1,t-j}, \dots, \hat{F}_{J,t-j})$. If $i = j$, the bottom right block is $\mathbf{0}_{J-K,J-K}$. Hence, the assertion is equivalent to

$$\frac{1}{T} \sum_{t=h+1}^T \hat{F}_{k,t-i} \hat{F}_{l,t-j} = O_P(T^{-1/2})$$

for all index combinations $k = K+1, \dots, J$, $l = 1, \dots, J$, and i, j that satisfy either $i \neq j$ or $l \leq K$. Using the notation $\check{F}_{l,t} = \langle Y_t - \mu, \hat{\psi}_l \rangle$ with $\hat{F}_{l,t} = \check{F}_{l,t} + \langle \mu - \hat{\mu}, \hat{\psi}_k \rangle$, Theorem 1(a) implies that it remains to show

$$\frac{1}{T} \sum_{t=h+1}^T \check{F}_{k,t-i} \check{F}_{l,t-j} = O_P(T^{-1/2}). \quad (\text{A.15})$$

Inserting the sign-adjusted model representation $Y_t = \mu + \sum_{m=1}^K \tilde{F}_{m,t} \tilde{\psi}_m + \epsilon_t^*$, we get, for any $l = 1, \dots, J$,

$$\check{F}_{l,t-j} = \langle Y_{t-j} - \mu, \hat{\psi}_l \rangle = \sum_{m=1}^K \tilde{F}_{m,t-j} \langle \tilde{\psi}_m, \hat{\psi}_l \rangle + \langle \epsilon_{t-j}^*, \hat{\psi}_l \rangle.$$

Since $k > K$, we have $\langle \hat{\psi}_m, \hat{\psi}_k \rangle = 0$, which yields

$$\check{F}_{k,t-i} = \sum_{m=1}^K \tilde{F}_{m,t-i} \langle \tilde{\psi}_m, \hat{\psi}_k \rangle + \langle \epsilon_{t-i}^*, \hat{\psi}_k \rangle = \sum_{m=1}^K \tilde{F}_{m,t-i} \langle \tilde{\psi}_m - \hat{\psi}_m, \hat{\psi}_k \rangle + \langle \epsilon_{t-i}^*, \hat{\psi}_k \rangle.$$

Hence, the left-hand-side of (A.15) is $T^{-1} \sum_{t=h+1}^T \check{F}_{k,t-i} \check{F}_{l,t-j} = H_1 + H_2 + H_3 + H_4$ with

$$\begin{aligned} H_1 &= \frac{1}{T} \sum_{t=h+1}^T \sum_{m_1, m_2=1}^K \tilde{F}_{m_1, t-i} \tilde{F}_{m_2, t-j} \langle \tilde{\psi}_{m_1} - \hat{\psi}_{m_1}, \hat{\psi}_k \rangle \langle \tilde{\psi}_{m_2}, \hat{\psi}_l \rangle, \\ H_2 &= \frac{1}{T} \sum_{t=h+1}^T \sum_{m=1}^K \tilde{F}_{m, t-i} \langle \tilde{\psi}_m - \hat{\psi}_m, \hat{\psi}_k \rangle \langle \epsilon_{t-j}^*, \hat{\psi}_l \rangle, \\ H_3 &= \frac{1}{T} \sum_{t=h+1}^T \sum_{m=1}^K \tilde{F}_{m, t-j} \langle \tilde{\psi}_m, \hat{\psi}_l \rangle \langle \epsilon_{t-i}^*, \hat{\psi}_k \rangle, \\ H_4 &= \frac{1}{T} \sum_{t=h+1}^T \langle \epsilon_{t-i}^*, \hat{\psi}_k \rangle \langle \epsilon_{t-j}^*, \hat{\psi}_l \rangle. \end{aligned}$$

In what follows, we will use the facts that the loadings and sample eigenfunctions are of unit norm and that all random variables have bounded fourth moments. Moreover, we will apply the Cauchy-Schwarz and the triangle inequality multiple times. For the first two summands, Theorem 1(e) implies

$$\begin{aligned} |H_1| &\leq \sum_{m_1, m_2=1}^K \left\| \tilde{\psi}_{m_1} - \hat{\psi}_{m_1} \right\| \cdot \left| \frac{1}{T} \sum_{t=h+1}^T \tilde{F}_{m_1, t-i} \tilde{F}_{m_2, t-j} \right| = O_P(T^{-1/2}), \\ |H_2| &\leq \sum_{m=1}^K \left\| \tilde{\psi}_m - \hat{\psi}_m \right\| \cdot \left| \frac{1}{T} \sum_{t=h+1}^T \tilde{F}_{m, t-i} \langle \epsilon_{t-j}^*, \hat{\psi}_l \rangle \right| = O_P(T^{-1/2}). \end{aligned}$$

For the third summand, we have

$$|H_3| \leq \sum_{m=1}^K \left| \frac{1}{T} \sum_{t=h+1}^T \tilde{F}_{m, t-j} \langle \epsilon_{t-i}^*, \hat{\psi}_k \rangle \right| \leq \sum_{m=1}^K \left\| \frac{1}{T} \sum_{t=h+1}^T \tilde{F}_{m, t-j} \epsilon_{t-i}^*(s) \right\|.$$

For $j \leq i$, Assumption 3(b) implies

$$E[|H_3|] \leq K \cdot \sup_{s \in [a, b]} E \left[\left\| \frac{1}{T} \sum_{t=h+1}^T \tilde{F}_{t-j} \epsilon_{t-i}^*(s) \right\|_2 \right] = O(T^{-1/2}),$$

and Markov's inequality implies $H_3 = O_P(T^{-1/2})$. For $j > i$, note that, by Assumption 1(a), ϵ_t^* as a martingale difference sequence with respect to $\{\epsilon_{t-1}^*, \tilde{F}_{t-1}, \epsilon_{t-2}^*, \tilde{F}_{t-2}, \dots\}$, which implies that $E[\tilde{F}_{m, t_1-j} \tilde{F}_{m, t_2-j} \epsilon_{t_1-i}^*(r) \epsilon_{t_2-i}^*(r)] = 0$ for any $t_2 < t_1$. Then, since the

fourth moments are bounded,

$$\begin{aligned}
H_3^2 &\leq \int_a^b \left(\frac{1}{T} \sum_{t=h+1}^T \tilde{F}_{m,t-j} \epsilon_{t-i}^*(r) \right)^2 dr \\
&= \int_a^b \frac{1}{T^2} \sum_{t=h+1}^T (\tilde{F}_{m,t-j} \epsilon_{t-i}^*(r))^2 dr + \int_a^b \frac{2}{T^2} \sum_{t_1=h+2}^T \sum_{t_2=h+1}^{t_1-1} \tilde{F}_{m,t_1-j} \tilde{F}_{m,t_2-j} \epsilon_{t_1-i}^*(r) \epsilon_{t_2-i}^*(r) dr \\
&= O_P(T^{-1}).
\end{aligned}$$

Finally, for the fourth summand, let us first consider the case $i \neq j$. Then,

$$\begin{aligned}
|H_4|^2 &\leq \left\| \frac{1}{T} \sum_{t=h+1}^T \epsilon_{t-i}^* \langle \epsilon_{t-j}^*, \hat{\psi}_l \rangle \right\|^2 \leq \int_a^b \int_a^b \left(\frac{1}{T} \sum_{t=h+1}^T \epsilon_{t-i}^*(r) \epsilon_{t-j}^*(s) \right)^2 ds dr \\
&= \int_a^b \int_a^b \frac{1}{T^2} \sum_{t=h+1}^T (\epsilon_{t-i}^*(r) \epsilon_{t-j}^*(s))^2 ds dr \\
&\quad + \int_a^b \int_a^b \frac{2}{T^2} \sum_{t_1=h+2}^T \sum_{t_2=h+1}^{t_1-1} \epsilon_{t_1-i}^*(r) \epsilon_{t_2-i}^*(r) \epsilon_{t_1-j}^*(s) \epsilon_{t_2-j}^*(s) ds dr \\
&= O_P(T^{-1}), \tag{A.16}
\end{aligned}$$

where the last step follows from the facts that ϵ_t^* has bounded fourth moments and satisfies $E[\epsilon_{t_1-i}^*(r) \epsilon_{t_2-i}^*(r) \epsilon_{t_1-j}^*(s) \epsilon_{t_2-j}^*(s)] = 0$ because of the martingale difference sequence property discussed above. Now let us consider $i = j$, where it must be the case that $j \leq K$ and $k > K$ as discussed at the beginning of this proof. Then, since $\langle \epsilon_{t-i}^*, \tilde{\psi}_l \rangle = 0$,

$$|H_4| = \left| \frac{1}{T} \sum_{t=h+1}^T \langle \epsilon_{t-i}^*, \hat{\psi}_k \rangle \langle \epsilon_{t-i}^*, \hat{\psi}_l - \tilde{\psi}_l \rangle \right| \leq \left\| \hat{\psi}_l - \tilde{\psi}_l \right\| \cdot \left\| \frac{1}{T} \sum_{t=h+1}^T \epsilon_{t-i}^* \langle \epsilon_{t-i}^*, \hat{\psi}_k \rangle \right\|,$$

which is $O_P(T^{-1/2})$ by Theorem 1(e). Finally, the triangle inequality implies (A.15), and the assertion follows.

A.10 Proof of Lemma A.4

A useful result for this proof is that, for any $j = 1, \dots, K$,

$$|\hat{F}_{l,t} - \tilde{F}_{l,t}| = |\langle Y_t - \mu, \hat{\psi}_l - \tilde{\psi}_l \rangle + \langle \hat{\mu} - \mu, \hat{\psi}_l \rangle| \leq \|Y_t - \mu\| \|\hat{\psi}_l - \tilde{\psi}_l\| + \|\hat{\mu} - \mu\|, \tag{A.17}$$

and, for any $j > K$,

$$\begin{aligned} |\widehat{F}_{l,t} - \langle \epsilon_t^*, \widehat{\psi}_l \rangle| &= |\langle Y_t - \widehat{\mu} - \epsilon_t^*, \widehat{\psi}_l \rangle| = \left| \langle \mu - \widehat{\mu}, \widehat{\psi}_l \rangle + \sum_{k=1}^K \widetilde{F}_{k,t} \langle \widetilde{\psi}_k, \widehat{\psi}_l \rangle \right| \\ &= \left| \langle \mu - \widehat{\mu}, \widehat{\psi}_l \rangle + \sum_{k=1}^K \widetilde{F}_{k,t} \langle \widetilde{\psi}_k - \widehat{\psi}_k, \widehat{\psi}_l \rangle \right| \leq \|\mu - \widehat{\mu}\| + \sum_{k=1}^K |\widetilde{F}_{k,t}| \|\widetilde{\psi}_k - \widehat{\psi}_k\|. \end{aligned} \quad (\text{A.18})$$

Proof of item (a): By the triangle inequality,

$$\begin{aligned} \left\| \frac{1}{T} \sum_{t=m+1}^T \widehat{\mathbf{x}}_{t-1}^{(J,m)} \eta'_t \right\|_M &\leq \sum_{i=1}^m \left\| \frac{1}{T} \sum_{t=m+1}^T \widehat{F}_{t-i}^{(J)} \eta'_t \right\|_M \\ &\leq \sum_{i=1}^m \left\| \frac{1}{T} \sum_{t=m+1}^T \widehat{F}_{t-i}^{(K)} \eta'_t \right\|_M + \sum_{i=1}^m \sum_{l=K+1}^J \sum_{h=1}^K \left| \frac{1}{T} \sum_{t=m+1}^T \widehat{F}_{l,t-i} \eta_{h,t} \right|. \end{aligned} \quad (\text{A.19})$$

For the first summand of (A.19), we have, for any $i = 1, \dots, m$,

$$\left\| \frac{1}{T} \sum_{t=m+1}^T \widehat{F}_{t-i}^{(K)} \eta'_t \right\|_M \leq \sum_{h,l=1}^K \left| \frac{1}{T} \sum_{t=m+1}^T (\widehat{F}_{l,t-i} - \widetilde{F}_{l,t-i}) \eta_{h,t} \right| + \left\| \frac{1}{T} \sum_{t=m+1}^T \widetilde{F}_{t-i} \eta'_t \right\|_M. \quad (\text{A.20})$$

The first summand of (A.20) is $O_P(T^{-1/2})$ by (A.17) and Theorem 1. For the second summand of (A.20), note that $\widetilde{F}_t = \sum_{j=0}^{\infty} B_j \eta_{t-j}$ for some B_j with $\sum_{j=0}^{\infty} \|B_j\|_M < \infty$ by Assumption 3(a). Then, by the triangle inequality,

$$\left\| \frac{1}{T} \sum_{t=m+1}^T \widetilde{F}_{t-i} \eta'_t \right\|_M \leq \sum_{j=0}^{\infty} \|B_j\|_M \sum_{h,k=1}^K \left| \frac{1}{T} \sum_{t=m+1}^T \eta_{h,t-i-j} \eta_{k,t} \right|,$$

and, by Assumption 3(a),

$$E \left[\left(\frac{1}{T} \sum_{t=m+1}^T \eta_{h,t-i-j} \eta_{l,t} \right)^2 \right] = \frac{1}{T^2} \sum_{t=m+1}^T E[\eta_{h,t-i-j}^2 \eta_{l,t}^2] = O(T^{-1})$$

since $E[\eta_{h,t_1-i-j} \eta_{l,t_1} \eta_{h,t_2-i-j} \eta_{l,t_2}] = 0$ for $t_1 \neq t_2$ due to the martingale difference sequence property of η_t . Therefore, the second summand of (A.20) is $O_P(T^{-1/2})$, and, consequently, the first summand of (A.19) is $O_P(T^{-1/2})$. For the second summand of (A.19),

$$\left| \frac{1}{T} \sum_{t=m+1}^T \widehat{F}_{l,t-i} \eta_{h,t} \right| \leq \left| \frac{1}{T} \sum_{t=m+1}^T (\widehat{F}_{l,t-i} - \langle \epsilon_{t-i}^*, \widehat{\psi}_l \rangle) \eta_{h,t} \right| + \left| \frac{1}{T} \sum_{t=m+1}^T \langle \epsilon_{t-i}^*, \widehat{\psi}_l \rangle \eta_{h,t} \right|. \quad (\text{A.21})$$

The first summand of the right-hand side of (A.21) is $O_P(T^{-1/2})$ by (A.18) and Theorem 1. For the second summand of (A.21), the Cauchy-Schwarz inequality yields

$$\left| \frac{1}{T} \sum_{t=m+1}^T \langle \epsilon_{t-i}^*, \hat{\psi}_l \rangle \eta_{h,t} \right| \leq \left\| \frac{1}{T} \sum_{t=m+1}^T \epsilon_{t-i}^* \eta_{h,t} \right\| = O_P(T^{-1/2}),$$

where the last step follows by Assumption 3(b) and the fact that $\eta_t = F_t^* - \sum_{j=1}^p A_j F_{t-j}^*$ by Assumption 3(a). Consequently, (A.19) is $O_P(T^{-1/2})$.

Proof of item (b): By the triangle inequality, we have

$$\sum_{l=1}^J \left\| \frac{1}{T} \sum_{t=m+1}^T \hat{\mathbf{x}}_{t-1}^{(J,m)} \langle \hat{\psi}_l, \epsilon_t^* \rangle \right\|_M \leq \sum_{h,l=1}^J \sum_{i=1}^m \left| \frac{1}{T} \sum_{t=m+1}^T \hat{F}_{h,t-i} \langle \hat{\psi}_l, \epsilon_t^* \rangle \right|.$$

and it remains to show that $T^{-1} \sum_{t=m+1}^T \hat{F}_{h,t-i} \langle \hat{\psi}_l, \epsilon_t^* \rangle = O_P(T^{-1/2})$ for any $i = 1, \dots, m$ and $h, l = 1, \dots, J$. We follow the same steps as in the proof of item (b) and first consider the case $h \leq K$, where

$$\left| \frac{1}{T} \sum_{t=m+1}^T \hat{F}_{h,t-i} \langle \hat{\psi}_l, \epsilon_t^* \rangle \right| \leq \left| \frac{1}{T} \sum_{t=m+1}^T (\hat{F}_{h,t-i} - \tilde{F}_{h,t-i}) \langle \hat{\psi}_l, \epsilon_t^* \rangle \right| + \left| \frac{1}{T} \sum_{t=m+1}^T \tilde{F}_{h,t-i} \langle \hat{\psi}_l, \epsilon_t^* \rangle \right|.$$

The first summand is $O_P(T^{-1/2})$ by (A.17) and Theorem 1, and the second summand is $O_P(T^{-1/2})$ since ϵ_t^* is a m.d.s. with respect to $\{\epsilon_{t-1}^*, \tilde{F}_{t-1}, \epsilon_{t-2}^*, \tilde{F}_{t-2}, \dots\}$. For the case $h > K$, we have

$$\left| \frac{1}{T} \sum_{t=m+1}^T \hat{F}_{h,t-i} \langle \hat{\psi}_l, \epsilon_t^* \rangle \right| \leq \left| \frac{1}{T} \sum_{t=m+1}^T (\hat{F}_{h,t-i} - \langle \epsilon_{t-i}^*, \hat{\psi}_h \rangle) \langle \hat{\psi}_l, \epsilon_t^* \rangle \right| + \left| \frac{1}{T} \sum_{t=m+1}^T \langle \epsilon_{t-i}^*, \hat{\psi}_h \rangle \langle \hat{\psi}_l, \epsilon_t^* \rangle \right|,$$

where the first summand is $O_P(T^{-1/2})$ by (A.18) and Theorem 1. The second summand is $O_P(T^{-1/2})$ analogously to (A.16) in the proof of Lemma A.3 because ϵ_t^* is a m.d.s. with respect to $\{\epsilon_{t-1}^*, \epsilon_{t-2}^*, \dots\}$.

Proof of item (c): By the Cauchy-Schwarz and the triangle inequality,

$$\begin{aligned} & \left\| \frac{1}{T} \sum_{t=m+1}^T \hat{\mathbf{x}}_{t-1}^{(J,m)} (\tilde{\mathbf{x}}_{t-1} - \hat{\mathbf{x}}_{t-1}^{(K,p)})' \right\|_M \leq \frac{1}{T} \sum_{t=m+1}^T \|\hat{\mathbf{x}}_{t-1}^{(J,m)}\|_2 \|\tilde{\mathbf{x}}_{t-1} - \hat{\mathbf{x}}_{t-1}^{(K,p)}\|_2 \\ & \leq \frac{1}{T} \sum_{t=m+1}^T \sum_{i=1}^p \sum_{l=1}^K \|\hat{\mathbf{x}}_{t-1}^{(J,m)}\|_2 |\tilde{F}_{l,t-i} - \hat{F}_{l,t-i}| = O_P(T^{-1/2}), \end{aligned}$$

where the last step follows from (A.17) and Theorem 1.

A.11 Proof of Lemma A.5

We denote the case overselection case ($J \geq K$ and $m \geq p$) as case I and the underselection case ($J < K$ or $m < p$ or both) as case II.

Proof of statement (a): From equation (A.3) the predictor curves have the representations

$$\hat{Y}_{t|t-1}^{(K,p)}(r) - \hat{\mu}(r) = (\hat{\Psi}^{(J^*)}(r))' \hat{\mathbf{A}}^* \hat{\mathbf{x}}_{t-1}^{(J^*,m^*)}$$

and

$$\begin{aligned} \hat{Y}_{t|t-1}^{(K,p)}(r) - \hat{\mu}(r) &= (\hat{\Psi}^{(K)}(r))' (\hat{\mathbf{A}}_{(K,p)} - \tilde{\mathbf{A}}) \hat{\mathbf{x}}_{t-1}^{(K,p)} + (\hat{\Psi}^{(K)}(r))' \tilde{\mathbf{A}} \hat{\mathbf{x}}_{t-1}^{(K,p)} \\ &= (\hat{\Psi}^{(K)}(r))' (\hat{\mathbf{A}}_{(K,p)} - \tilde{\mathbf{A}}) \hat{\mathbf{x}}_{t-1}^{(K,p)} + (\hat{\Psi}^{(J^*)}(r))' \mathbf{A}^* \hat{\mathbf{x}}_{t-1}^{(J^*,m^*)}. \end{aligned}$$

Then, $\hat{Y}_{t|t-1}^{(K,p)}(r) - \hat{Y}_{t|t-1}^{(J,m)}(r) = Z_{(1)}(r) + Z_{(2)}(r)$, where

$$Z_{(1)}(r) = (\hat{\Psi}^{(J^*)}(r))' (\mathbf{A}^* - \hat{\mathbf{A}}^*) \hat{\mathbf{x}}_{t-1}^{(J^*,m^*)}, \quad Z_{(2)}(r) = (\hat{\Psi}^{(K)}(r))' (\hat{\mathbf{A}}_{(K,p)} - \tilde{\mathbf{A}}) \hat{\mathbf{x}}_{t-1}^{(K,p)}. \quad (\text{A.22})$$

To simplify the exposition we ignore the additional indices $\{t, T, J, m, K, p\}$ on which $Z_{(1)}$ and $Z_{(2)}$ depend. To disentangle the loading vectors and matrix products, let $e_l^{(J)}$ be the l -th unit vector of length J , where the l -th entry of $e_l^{(J)}$ is 1, and all other entries are zeros. For the first term, we have

$$\begin{aligned} \|Z_{(1)}\|^2 &= \int_a^b \left(\sum_{l=1}^{J^*} \hat{\psi}_l(r) (e_l^{(J^*)})' (\mathbf{A}^* - \hat{\mathbf{A}}^*) \hat{\mathbf{x}}_{t-1}^{(J^*,m^*)} \right)^2 dr \\ &= \sum_{l=1}^{J^*} \left((e_l^{(J^*)})' (\mathbf{A}^* - \hat{\mathbf{A}}^*) \hat{\mathbf{x}}_{t-1}^{(J^*,m^*)} \right)^2 \\ &= \|(\mathbf{A}^* - \hat{\mathbf{A}}^*) \hat{\mathbf{x}}_{t-1}^{(J^*,m^*)}\|_M^2 \\ &= \text{tr} \left((\hat{\mathbf{x}}_{t-1}^{(J^*,m^*)})' (\mathbf{A}^* - \hat{\mathbf{A}}^*)' (\mathbf{A}^* - \hat{\mathbf{A}}^*) \hat{\mathbf{x}}_{t-1}^{(J^*,m^*)} \right) \\ &= \text{tr} \left((\mathbf{A}^* - \hat{\mathbf{A}}^*)' (\mathbf{A}^* - \hat{\mathbf{A}}^*) \hat{\mathbf{x}}_{t-1}^{(J^*,m^*)} (\hat{\mathbf{x}}_{t-1}^{(J^*,m^*)})' \right), \end{aligned}$$

and

$$\frac{1}{T} \sum_{t=m^*+1}^T \|Z_{(1)}\|^2 = \text{tr} \left((\mathbf{A}^* - \hat{\mathbf{A}}^*)' (\mathbf{A}^* - \hat{\mathbf{A}}^*) \hat{\Sigma}_{(J^*,m^*)} \right).$$

From the proof of Theorem 2, $\|\hat{\Sigma}_{(J^*,m^*)} - \tilde{\Sigma}^*\|_M = o_P(1)$ and $\|\hat{\Sigma}_{(J^*,m^*)}^{-1} - (\tilde{\Sigma}^*)^{-1}\|_M = o_P(1)$. Consider the Cholesky decompositions $\hat{\Sigma}_{(J^*,m^*)} = \hat{\Omega} \hat{\Omega}'$ and $\tilde{\Sigma}^* = \Omega \Omega'$, where $\|\Omega\|_M < \infty$

and $\|\Omega^{-1}\|_M < \infty$. Then,

$$\text{tr} \left((\mathbf{A}^* - \hat{\mathbf{A}}^*)' (\mathbf{A}^* - \hat{\mathbf{A}}^*) \hat{\Sigma}_{(J^*, m^*)} \right) = \|(\mathbf{A}^* - \hat{\mathbf{A}}^*) \hat{\Omega}\|_M^2,$$

and

$$\begin{aligned} \frac{\|(\mathbf{A}^* - \hat{\mathbf{A}}^*) \hat{\Omega}\|_M^2}{\|\mathbf{A}^* - \hat{\mathbf{A}}^*\|_M^2} &\leq \|\hat{\Omega}\|_M^2 = O_P(1), \\ \frac{\|\mathbf{A}^* - \hat{\mathbf{A}}^*\|_M^2}{\|(\mathbf{A}^* - \hat{\mathbf{A}}^*) \hat{\Omega}\|_M^2} &= \frac{\|(\mathbf{A}^* - \hat{\mathbf{A}}^*) \hat{\Omega} \hat{\Omega}^{-1}\|_M^2}{\|(\mathbf{A}^* - \hat{\mathbf{A}}^*) \hat{\Omega}\|_M^2} \leq \|\hat{\Omega}^{-1}\|_M^2 = O_P(1), \end{aligned}$$

which implies that $T^{-1} \sum_{t=m^*+1}^T \|Z_{(1)}\|^2$ is of exactly the same order as $\|\mathbf{A}^* - \hat{\mathbf{A}}^*\|_M^2$. By Theorem 2, we have $\|\mathbf{A}^* - \hat{\mathbf{A}}^*\|_M^2 = O_P(T^{-1})$ for case I and $\|\mathbf{A}^* - \hat{\mathbf{A}}^*\|_M^2 = \Theta_P(1)$ for case II, which implies that

$$\frac{1}{T} \sum_{t=m^*+1}^T \|Z_{(1)}\|^2 = \begin{cases} O_P(T^{-1}) & \text{for case I,} \\ \Theta_P(1) & \text{for case II.} \end{cases}$$

For the second term, by the orthonormality of the loadings,

$$\|Z_{(2)}\|^2 = \|(\hat{\mathbf{A}}_{(K,p)} - \tilde{\mathbf{A}}) \hat{\mathbf{x}}_{t-1}^{(K,p)}\|_M^2 \leq \|\hat{\mathbf{A}}_{(K,p)} - \tilde{\mathbf{A}}\|_M^2 \|\hat{\mathbf{x}}_{t-1}^{(K,p)}\|_M^2,$$

and, for both cases,

$$\frac{1}{T} \sum_{t=m^*+1}^T \|Z_{(2)}\|^2 \leq \frac{1}{T} \sum_{t=m^*+1}^T \|\hat{\mathbf{x}}_{t-1}^{(K,p)}\|_M^2 \|\hat{\mathbf{A}}_{(K,p)} - \tilde{\mathbf{A}}\|_M^2 = O_P(T^{-1})$$

by Theorem 2 and the fact that enough moments are bounded. Finally, for the cross term,

$$\frac{1}{T} \sum_{t=m^*+1}^T \langle Z_{(1)}, Z_{(2)} \rangle \leq \frac{1}{T} \sum_{t=m^*+1}^T \|\hat{\mathbf{x}}_{t-1}^{(K,p)}\|_2 \|\hat{\mathbf{x}}_{t-1}^{(J,m)}\|_M \|\hat{\mathbf{A}}_{(K,p)} - \tilde{\mathbf{A}}\|_M \|\mathbf{A}^* - \hat{\mathbf{A}}^*\|_2,$$

which is $O_P(T^{-1})$ for case I and $O_P(T^{-1/2})$ for case II by Theorem 2. Since

$$\frac{1}{T} \sum_{t=m^*+1}^T \|\hat{Y}_{t|t-1}^{(K,p)} - \hat{Y}_{t|t-1}^{(J,m)}\|^2 = \frac{1}{T} \sum_{t=m^*+1}^T (\|Z_{(1)}\|^2 + \|Z_{(2)}\|^2 + 2\langle Z_{(1)}, Z_{(2)} \rangle),$$

statement (a) follows.

Proof of statement (b): From equations (A.2) and (A.4), it follows that

$$Y_t(r) - \tilde{Y}_{t|t-1}(r) = Z_{(3)}(r) + Z_{(4)}(r), \quad Z_{(3)}(r) = (\tilde{\Psi}(r))' \eta_t, \quad Z_{(4)}(r) = \epsilon_t^*(r).$$

where $Z_{(3)}(r) = \Psi' \eta_t$, and $Z_{(5)} = \epsilon_t$. Using the definitions of $Z_{(1)}$ and $Z_{(2)}$ in (A.22), by Theorem 2 it remains to show that

$$\frac{1}{T} \sum_{t=m^*+1}^T \langle Z_{(1)} + Z_{(2)}, Z_{(3)} + Z_{(4)} \rangle = O_P(T^{-1/2} \|\mathbf{A}^* - \hat{\mathbf{A}}^*\|_M).$$

We consider the four terms $\langle Z_{(i)}, Z_{(j)} \rangle$ for $i = 1, 2$ and $j = 3, 4$ separately. For the first term, by the properties of the trace,

$$\begin{aligned} \langle Z_{(1)}, Z_{(3)} \rangle &= \int_a^b \eta'_t(\tilde{\Psi}(r))(\hat{\Psi}^{(J^*)}(r))'(\mathbf{A}^* - \hat{\mathbf{A}}^*)\hat{\mathbf{x}}_{t-1}^{(J^*, m^*)} dr \\ &= \text{tr} \left(\left(\int_a^b (\tilde{\Psi}(r))(\hat{\Psi}^{(J^*)}(r))' dr \right) (\mathbf{A}^* - \hat{\mathbf{A}}^*)\hat{\mathbf{x}}_{t-1}^{(J^*, m^*)} \eta'_t \right), \end{aligned}$$

and, by the Cauchy-Schwarz inequality for the trace,

$$\frac{1}{T} \sum_{t=m^*+1}^T \langle Z_{(1)}, Z_{(3)} \rangle \leq \|\mathbf{A}^* - \hat{\mathbf{A}}^*\|_M \left\| \frac{1}{T} \sum_{t=m^*+1}^T \hat{\mathbf{x}}_{t-1}^{(J^*, m^*)} \eta'_t \right\|_M = O_P(T^{-1/2} \|\mathbf{A}^* - \hat{\mathbf{A}}^*\|_M),$$

where the last step follows from Lemma A.4(a). Analogously, for the second term,

$$\begin{aligned} \langle Z_{(2)}, Z_{(3)} \rangle &= \int_a^b \eta'_t(\tilde{\Psi}(r))(\hat{\Psi}^{(K)}(r))'(\hat{\mathbf{A}}_{(K,p)} - \tilde{\mathbf{A}})\hat{\mathbf{x}}_{t-1}^{(K,p)} dr \\ &= \text{tr} \left(\left(\int_a^b (\tilde{\Psi}(r))(\hat{\Psi}^{(K)}(r))' dr \right) (\hat{\mathbf{A}}_{(K,p)} - \tilde{\mathbf{A}})\hat{\mathbf{x}}_{t-1}^{(K,p)} \eta'_t \right), \end{aligned}$$

and

$$\frac{1}{T} \sum_{t=m^*+1}^T \langle Z_{(2)}, Z_{(3)} \rangle \leq \|\hat{\mathbf{A}}_{(K,p)} - \tilde{\mathbf{A}}\|_M \left\| \frac{1}{T} \sum_{t=m^*+1}^T \hat{\mathbf{x}}_{t-1}^{(K,p)} \eta'_t \right\|_M = O_P(T^{-1/2} \|\mathbf{A}^* - \hat{\mathbf{A}}^*\|_M).$$

For the third term, we have

$$\begin{aligned} \langle Z_{(1)}, Z_{(4)} \rangle &= \int_a^b \epsilon_t^*(r)(\hat{\Psi}^{(J^*)}(r))'(\mathbf{A}^* - \hat{\mathbf{A}}^*)\hat{\mathbf{x}}_{t-1}^{(J^*, m^*)} dr \\ &= \text{tr} \left((\mathbf{A}^* - \hat{\mathbf{A}}^*) \sum_{l=1}^{J^*} \hat{\mathbf{x}}_{t-1}^{(J^*, m^*)} \langle \epsilon_t^*, \hat{\psi}_l \rangle \right), \end{aligned}$$

and

$$\frac{1}{T} \sum_{t=m^*+1}^T \langle Z_{(1)}, Z_{(4)} \rangle \leq \|\mathbf{A}^* - \hat{\mathbf{A}}^*\|_M \left\| \frac{1}{T} \sum_{t=m^*+1}^T \sum_{l=1}^{J^*} \hat{\mathbf{x}}_{t-1}^{(J^*, m^*)} \langle \epsilon_t^*, \hat{\psi}_l \rangle \right\|_M,$$

which is $O_P(T^{-1/2}\|\mathbf{A}^* - \hat{\mathbf{A}}^*\|_M)$ by Lemma A.4(b). Finally, for the fourth term,

$$\begin{aligned}\langle Z_{(2)}, Z_{(4)} \rangle &= \int_a^b \epsilon_t^*(r) (\hat{\Psi}^{(K)}(r))' (\hat{\mathbf{A}}_{(K,p)} - \tilde{\mathbf{A}}) \hat{\mathbf{x}}_{t-1}^{(K,p)} dr \\ &= \text{tr} \left((\hat{\mathbf{A}}_{(K,p)} - \tilde{\mathbf{A}}) \sum_{l=1}^K \hat{\mathbf{x}}_{t-1}^{(K,p)} \langle \epsilon_t^*, \hat{\psi}_l \rangle \right),\end{aligned}$$

and

$$\frac{1}{T} \sum_{t=m^*+1}^T \langle Z_{(2)}, Z_{(4)} \rangle \leq \|\hat{\mathbf{A}}_{(K,p)} - \tilde{\mathbf{A}}\|_M \left\| \frac{1}{T} \sum_{t=m^*+1}^T \sum_{l=1}^K \hat{\mathbf{x}}_{t-1}^{(K,p)} \langle \epsilon_t^*, \hat{\psi}_l \rangle \right\|_M,$$

which is $O_P(T^{-1/2}\|\mathbf{A}^* - \hat{\mathbf{A}}^*\|_M)$ by Lemma A.4(b) as well.

Proof of statement (c): We decompose

$$\begin{aligned}\tilde{Y}_{t|t-1}(r) - \hat{Y}_{t|t-1}^{(K,p)}(r) &= \mu(r) + (\tilde{\Psi}(r))' \tilde{\mathbf{A}} \tilde{\mathbf{x}}_{t-1} - \hat{\mu}(r) - (\hat{\Psi}^{(K)}(r))' \hat{\mathbf{A}}_{(K,p)} \hat{\mathbf{x}}_{t-1}^{(K,p)} \\ &= Z_{(5)}(r) + Z_{(6)}(r) + Z_{(7)}(r) + Z_{(8)}(r),\end{aligned}$$

where

$$\begin{aligned}Z_{(5)}(r) &= \mu(r) - \hat{\mu}(r), \quad Z_{(6)}(r) = (\tilde{\Psi}(r) - \hat{\Psi}^{(K)}(r))' \tilde{\mathbf{A}} \tilde{\mathbf{x}}_{t-1}, \\ Z_{(7)}(r) &= (\hat{\Psi}^{(K)}(r))' (\tilde{\mathbf{A}} - \hat{\mathbf{A}}_{(K,p)}) \tilde{\mathbf{x}}_{t-1}, \quad Z_{(8)}(r) = (\hat{\Psi}^{(K)}(r))' \hat{\mathbf{A}}_{(K,p)} (\tilde{\mathbf{x}}_{t-1} - \hat{\mathbf{x}}_{t-1}^{(K,p)}).\end{aligned}$$

It remains to show that

$$\frac{1}{T} \sum_{t=m^*+1}^T \langle Z_{(1)} + Z_{(2)}, Z_{(5)} + Z_{(6)} + Z_{(7)} + Z_{(8)} \rangle = O_P(T^{-1/2}\|\mathbf{A}^* - \hat{\mathbf{A}}^*\|_M).$$

We consider the four terms $\langle Z_{(1)} + Z_{(2)}, Z_{(j)} \rangle$ for $j = 5, 6, 7, 8$ separately. First, from the proof of statement (a),

$$\frac{1}{T} \sum_{t=m^*+1}^T (\|Z_{(1)}\| + \|Z_{(2)}\|) = O_P(\|\mathbf{A}^* - \hat{\mathbf{A}}^*\|_M),$$

which, together with Theorem 1(a), implies that

$$\begin{aligned}\left| \frac{1}{T} \sum_{t=m^*+1}^T \langle Z_{(1)} + Z_{(2)}, Z_{(5)} \rangle \right| &\leq \frac{1}{T} \sum_{t=m^*+1}^T (\|Z_{(1)}\| + \|Z_{(2)}\|) \|\mu - \hat{\mu}\| \\ &= O_P(T^{-1/2}\|\mathbf{A}^* - \hat{\mathbf{A}}^*\|_M).\end{aligned}$$

For the second term, by the Cauchy-Schwarz inequality and the orthonormality of the loadings, we have

$$\begin{aligned}
\langle Z_{(1)}, Z_{(6)} \rangle &= \text{tr} \left(\int_a^b (\hat{\mathbf{x}}_{t-1}^{(J^*, m^*)})' (\mathbf{A}^* - \hat{\mathbf{A}}^*)' (\hat{\Psi}^{(J^*)}(r)) (\tilde{\Psi}(r) - \hat{\Psi}^{(K)}(r))' \tilde{\mathbf{A}} \tilde{\mathbf{x}}_{t-1} \, dr \right) \\
&\leq \|\tilde{\mathbf{A}} \tilde{\mathbf{x}}_{t-1} (\hat{\mathbf{x}}_{t-1}^{(J^*, m^*)})'\|_M \|\mathbf{A}^* - \hat{\mathbf{A}}^*\|_M \sum_{l=1}^K \|\tilde{\psi}_l - \hat{\psi}_l\| \\
\langle Z_{(2)}, Z_{(6)} \rangle &= \text{tr} \left(\int_a^b (\hat{\mathbf{x}}_{t-1}^{(K, p)})' (\hat{\mathbf{A}}_{(K, p)} - \tilde{\mathbf{A}})' (\hat{\Psi}^{(K)}(r)) (\tilde{\Psi}(r) - \hat{\Psi}^{(K)}(r))' \tilde{\mathbf{A}} \tilde{\mathbf{x}}_{t-1} \, dr \right) \\
&\leq \|\tilde{\mathbf{A}} \tilde{\mathbf{x}}_{t-1} (\hat{\mathbf{x}}_{t-1}^{(K, p)})'\|_M \|\hat{\mathbf{A}}_{(K, p)} - \tilde{\mathbf{A}}\|_M \sum_{l=1}^K \|\tilde{\psi}_l - \hat{\psi}_l\|,
\end{aligned}$$

and Theorem 1(e) implies

$$\left| \frac{1}{T} \sum_{t=m^*+1}^T \langle Z_{(1)} + Z_{(2)}, Z_{(6)} \rangle \right| = O_P(T^{-1/2} \|\mathbf{A}^* - \hat{\mathbf{A}}^*\|_M).$$

For the third term,

$$\begin{aligned}
\langle Z_{(1)}, Z_{(7)} \rangle &= \text{tr} \left(\int_a^b (\hat{\mathbf{x}}_{t-1}^{(J^*, m^*)})' (\mathbf{A}^* - \hat{\mathbf{A}}^*)' (\hat{\Psi}^{(J^*)}(r)) (\hat{\Psi}^{(K)}(r))' (\tilde{\mathbf{A}} - \hat{\mathbf{A}}_{(K, p)}) \tilde{\mathbf{x}}_{t-1} \, dr \right) \\
&\leq K \|\mathbf{A}^* - \hat{\mathbf{A}}^*\|_M \|\tilde{\mathbf{A}} - \hat{\mathbf{A}}_{(K, p)}\|_M \|\tilde{\mathbf{x}}_{t-1} (\hat{\mathbf{x}}_{t-1}^{(J^*, m^*)})'\|_M, \\
\langle Z_{(2)}, Z_{(7)} \rangle &= \text{tr} \left(\int_a^b (\hat{\mathbf{x}}_{t-1}^{(K, p)})' (\hat{\mathbf{A}}_{(K, p)} - \tilde{\mathbf{A}})' (\hat{\Psi}^{(K)}(r)) (\hat{\Psi}^{(K)}(r))' (\tilde{\mathbf{A}} - \hat{\mathbf{A}}_{(K, p)}) \tilde{\mathbf{x}}_{t-1} \, dr \right) \\
&\leq K \|\tilde{\mathbf{A}} - \hat{\mathbf{A}}_{(K, p)}\|_M^2 \|\tilde{\mathbf{x}}_{t-1} (\hat{\mathbf{x}}_{t-1}^{(K, p)})'\|_M,
\end{aligned}$$

and Theorem 2 implies

$$\frac{1}{T} \sum_{t=m^*+1}^T \langle Z_{(1)} + Z_{(2)}, Z_{(7)} \rangle = O_P(T^{-1/2} \|\mathbf{A}^* - \hat{\mathbf{A}}^*\|_M).$$

Finally, for the fourth term,

$$\begin{aligned}
\langle Z_{(1)}, Z_{(8)} \rangle &= \text{tr} \left(\int_a^b (\hat{\mathbf{x}}_{t-1}^{(J^*, m^*)})' (\mathbf{A}^* - \hat{\mathbf{A}}^*)' (\hat{\Psi}^{(J^*)}(r)) (\hat{\Psi}^{(K)}(r))' \hat{\mathbf{A}}_{(K, p)} (\tilde{\mathbf{x}}_{t-1} - \hat{\mathbf{x}}_{t-1}^{(K, p)}) \, dr \right) \\
\langle Z_{(2)}, Z_{(8)} \rangle &= \text{tr} \left(\int_a^b (\hat{\mathbf{x}}_{t-1}^{(K, p)})' (\hat{\mathbf{A}}_{(K, p)} - \tilde{\mathbf{A}})' (\hat{\Psi}^{(K)}(r)) (\hat{\Psi}^{(K)}(r))' \hat{\mathbf{A}}_{(K, p)} (\tilde{\mathbf{x}}_{t-1} - \hat{\mathbf{x}}_{t-1}^{(K, p)}) \, dr \right)
\end{aligned}$$

and

$$\begin{aligned} & \frac{1}{T} \sum_{t=m^*+1}^T \langle Z_{(1)} + Z_{(2)}, Z_{(8)} \rangle \\ & \leq 2K \left\| \frac{1}{T} \sum_{t=m^*+1}^T (\tilde{\mathbf{x}}_{t-1} - \hat{\mathbf{x}}_{t-1}^{(K,p)}) (\hat{\mathbf{x}}_{t-1}^{(J^*,m^*)})' \right\|_M \|\mathbf{A}^* - \hat{\mathbf{A}}^*\|_M \|\hat{\mathbf{A}}_{(K,p)}\|_M, \end{aligned}$$

which is $O_P(T^{-1/2} \|\mathbf{A}^* - \hat{\mathbf{A}}^*\|_M)$ by Lemma A.4(c).

References

- Aue, A., Norinho, D. D., and Hörmann, S. (2015). On the prediction of stationary functional time series. *Journal of the American Statistical Association*, 110:378–392.
- Bai, J. (2003). Inferential theory for factor models of large dimensions. *Econometrica*, 71:135–171.
- Bai, J. and Ng, S. (2002). Determining the number of factors in approximate factor models. *Econometrica*, 70:191–221.
- Bai, J. and Ng, S. (2008). Large dimensional factor analysis. *Foundations and Trends in Econometrics*, 3:89–163.
- Bai, J. and Ng, S. (2013). Principal components estimation and identification of static factors. *Journal of Econometrics*, 176:18–29.
- Bardsley, P., Horváth, L., Kokoszka, P., and Young, G. (2017). Change point tests in functional factor models with application to yield curves. *The Econometrics Journal*, 20:86–117.
- Bathia, N., Yao, Q., and Ziegelmann, F. (2010). Identifying the finite dimensionality of curve time series. *The Annals of Statistics*, 38:3352–3386.
- Berk, K. N. (1974). Consistent autoregressive spectral estimates. *The Annals of Statistics*, 2:489–502.
- Breitung, J. and Choi, I. (2013). Factor models. In *Handbook of Research Methods and Applications in Empirical Macroeconomics*, pages 249–265. Edward Elgar Publishing.
- Caldeira, J. F., Cordeiro, W. C., Ruiz, E., and Santos, A. A. (2025). Forecasting the yield curve: the role of additional and time-varying decay parameters, conditional heteroscedasticity, and macro-economic factors. *Journal of Time Series Analysis*, 46:258–285.

- Chamberlain, G. and Rothschild, M. (1983). Arbitrage, factor structure and mean-variance analysis in large asset markets. *Econometrica*, 51:1305–1324.
- Chang, Y., Kim, C. S., and Park, J. Y. (2016). Nonstationarity in time series of state densities. *Journal of Econometrics*, 192:152 – 167.
- Christensen, J. H., Diebold, F. X., and Rudebusch, G. D. (2009). An arbitrage-free generalized Nelson-Siegel term structure model. *The Econometrics Journal*, 12:C33–C64.
- Descary, M.-H. and Panaretos, V. M. (2019). Functional data analysis by matrix completion. *The Annals of Statistics*, 47:1–38.
- Diebold, F. X. and Li, C. (2006). Forecasting the term structure of government bond yields. *Journal of Econometrics*, 130:337–364.
- Diebold, F. X. and Rudebusch, G. D. (2013). *Yield curve modeling and forecasting: The dynamic Nelson-Siegel approach*. Princeton University Press.
- Diks, C. and Wouters, B. (2023). Noise reduction for functional time series. *arXiv preprint arXiv:2307.02154*.
- Forni, M., Hallin, M., Lippi, M., and Reichlin, L. (2000). The generalized dynamic-factor model: Identification and estimation. *Review of Economics and Statistics*, 82:540–554.
- Hall, P., Müller, H.-G., and Wang, J.-L. (2006). Properties of principal component methods for functional and longitudinal data analysis. *The Annals of Statistics*, 34:1493–1517.
- Hallin, M. and Liška, R. (2007). Determining the number of factors in the general dynamic factor model. *Journal of the American Statistical Association*, 102:603–617.
- Hallin, M., Nisol, G., and Tavakoli, S. (2023). Factor models for high-dimensional functional time series I: Representation results. *Journal of Time Series Analysis*, 44:578–600.
- Hays, S., Shen, H., and Huang, J. Z. (2012). Functional dynamic factor models with application to yield curve forecasting. *The Annals of Applied Statistics*, 6:870–894.
- Horváth, L. and Kokoszka, P. (2012). *Inference for functional data with applications*. Springer.
- Horváth, L., Kokoszka, P., VanderDoes, J., and Wang, S. (2022). Inference in functional factor models with applications to yield curves. *Journal of Time Series Analysis*, 43:872–894.

- Hsing, T. and Eubank, R. (2015). *Theoretical foundations of functional data analysis, with an introduction to linear operators*. John Wiley & Sons.
- Hyndman, R. J. and Shang, H. L. (2009). Forecasting functional time series. *Journal of the Korean Statistical Society*, 38:199–211.
- Hyndman, R. J. and Ullah, M. S. (2007). Robust forecasting of mortality and fertility rates: a functional data approach. *Computational Statistics & Data Analysis*, 51:4942–4956.
- Hörmann, S. and Jammoul, F. (2022). Consistently recovering the signal from noisy functional data. *Journal of Multivariate Analysis*, 189:104886.
- Hörmann, S. and Jammoul, F. (2023). Prediction in functional regression with discretely observed and noisy covariates. *Computational Statistics & Data Analysis*, 178:107600.
- Hörmann, S., Kidziński, L., and Hallin, M. (2015). Dynamic functional principal components. *Journal of the Royal Statistical Society: Series B (Statistical Methodology)*, 77:319–348.
- Hörmann, S. and Kokoszka, P. (2010). Weakly dependent functional data. *The Annals of Statistics*, 38:1845–1884.
- Kneip, A. and Liebl, D. (2020). On the optimal reconstruction of partially observed functional data. *The Annals of Statistics*, 48:1692–1717.
- Kokoszka, P. and Reimherr, M. (2017). *Introduction to Functional Data Analysis*. CRC Press.
- Kowal, D. R. and Canale, A. (2023). Semiparametric Functional Factor Models with Bayesian Rank Selection. *Bayesian Analysis*, 18:1161 – 1189.
- Kowal, D. R., Matteson, D. S., and Ruppert, D. (2017). A bayesian multivariate functional dynamic linear model. *Journal of the American Statistical Association*, 112:733–744.
- Lam, C. and Yao, Q. (2012). Factor modeling for high-dimensional time series: Inference for the number of factors. *The Annals of Statistics*, 40:694–726.
- Lengwiler, Y. and Lenz, C. (2010). Intelligible factors for the yield curve. *Journal of Econometrics*, 157:481–491.
- Li, D., Robinson, P. M., and Shang, H. L. (2020). Long-range dependent curve time series. *Journal of the American Statistical Association*, 115:957–971.

- Li, Y. and Hsing, T. (2010). Uniform convergence rates for nonparametric regression and principal component analysis in functional/longitudinal data. *The Annals of Statistics*, 38:3321–3351.
- Liebl, D. (2013). Modeling and forecasting electricity spot prices: A functional data perspective. *The Annals of Applied Statistics*, 7:1562–1592.
- Liu, Y. and Wu, J. C. (2021). Reconstructing the yield curve. *Journal of Financial Economics*, 142:1395–1425.
- Lütkepohl, H. (1996). *Handbook of Matrices*. Wiley.
- Montagna, S., Tokdar, S. T., Neelon, B., and Dunson, D. B. (2012). Bayesian latent factor regression for functional and longitudinal data. *Biometrics*, 68:1064–1073.
- Nelson, C. R. and Siegel, A. F. (1987). Parsimonious modeling of yield curves. *The Journal of Business*, 60:473–489.
- Nielsen, M. Ø., Seo, W.-K., and Seong, D. (2024). Inference on common trends in functional time series. *arXiv preprint arXiv:2312.00590v4*.
- Ofner, M. and Hörmann, S. (2024). Covariate-informed reconstruction of partially observed functional data via factor models. *arXiv preprint arXiv:2305.13152v3*.
- Panaretos, V. M. and Tavakoli, S. (2013). Fourier analysis of stationary time series in function space. *The Annals of Statistics*, 41:568–603.
- Pena, D. and Box, G. E. (1987). Identifying a simplifying structure in time series. *Journal of the American statistical Association*, 82:836–843.
- Ramsay, J. and Silverman, B. (2005). *Functional data analysis*. Springer.
- Salish, N. and Gleim, A. (2019). A moment-based notion of time dependence for functional time series. *Journal of Econometrics*, 212:377–392.
- Sen, R. and Klüppelberg, C. (2019). Time series of functional data with application to yield curves. *Applied Stochastic Models in Business and Industry*, 35:1028–1043.
- Stock, J. H. and Watson, M. W. (2002a). Forecasting using principal components from a large number of predictors. *Journal of the American Statistical Association*, 97:1167–1179.
- Stock, J. H. and Watson, M. W. (2002b). Macroeconomic forecasting using diffusion indexes. *Journal of Business & Economic Statistics*, 20:147–162.

- Stock, J. H. and Watson, M. W. (2016). Dynamic factor models, factor-augmented vector autoregressions, and structural vector autoregressions in macroeconomics. In *Handbook of Macroeconomics*, volume 2, pages 415–525. Elsevier.
- Svensson, L. E. (1995). Estimating forward interest rates with the extended nelson & siegel method. *Sveriges Riksbank Quarterly Review*, 3:13–26.
- Tavakoli, S., Nisol, G., and Hallin, M. (2023). Factor models for high-dimensional functional time series II: Estimation and forecasting. *Journal of Time Series Analysis*, 44:601–621.
- White, H. (2001). *Asymptotic Theory for Econometricians, revised edition*. Academic Press.
- Yao, F., Müller, H.-G., and Wang, J.-L. (2005). Functional data analysis for sparse longitudinal data. *Journal of the American Statistical Association*, 100:577–590.
- Zhang, R., Robinson, P., and Yao, Q. (2019). Identifying cointegration by eigenanalysis. *Journal of the American Statistical Association*, 114:916–927.
- Zhang, X. and Wang, J.-L. (2016). From sparse to dense functional data and beyond. *The Annals of Statistics*, 44:2281–2321.